

**RESEARCH ARTICLE**

WILEY

Impact of gully incision on hillslope hydrology

Xing Chen^{1,2} | Mukesh Kumar³ | Daniel deB Richter¹ | Yair Mau⁴¹Nicholas School of the Environment, Duke University, Durham, North Carolina²Rays Computational Intelligence Laboratory, Beijing Inteliway Environmental Science & Technology, Ltd., Beijing, 100191, China³Department of Civil, Construction, and Environmental Engineering, University of Alabama, Tuscaloosa, Alabama⁴The Department of Soil and Water Sciences, The Hebrew University of Jerusalem, Jerusalem, Israel**Correspondence**Mukesh Kumar, Department of Civil, Construction, and Environmental Engineering, University of Alabama, Tuscaloosa, AL.
Email: mukesh.kumar@ua.edu**Funding information**

National Science Foundation, Grant/Award Numbers: EAR-1331846, EAR-1856054, EAR-1920425

Abstract

The Southern U.S. Piedmont ranging from Virginia to Georgia underwent severe gully erosion over a century of farming mainly for cotton (1800s–1930s). Although tree succession blanketed much of this region by the middle 20th century, gully erosion still occurs, especially during wet seasons. While many studies on gully erosion have focused on soil loss, soil carbon exchange, and stormwater response, the impacts on soil moisture, groundwater, and transpiration remain under-studied. Using a newly developed 2D hydrologic model, this study analyzes the impacts of gully erosion on hillslope hydrologic states and fluxes. Results indicate that increases in gully incision lead to reduction in groundwater table, root zone soil moisture, and transpiration. These reductions show seasonal variations, but the season when the reduction is maximum differs among the hydrologic variables. Spatially, the impacts are generally the greatest near the toe of the hillslope and reduce further away from it, although the reductions are sometimes non-monotonic. Overall, the impacts are larger for shallow gully depths and diminish as the incision goes deeper. Lastly, the extent of impacts on a heterogeneous hillslope is found to be very different with respect to a homogeneous surrogate made of dominant soil properties. These results show that through gully erosion, the landscape not only loses soil but also a large amount of water from the subsurface. The magnitude of water loss is, however, dependent on hydrogeologic and topographic configuration of the hillslope. The results will facilitate (a) mapping of relative susceptibility of landscapes to gully erosion, (b) understanding of the impacts of stream manipulations such as due to dredging on hillslope ecohydrology, (c) prioritization of mitigation measures to prevent gully erosion, and (d) design of observation campaigns to assess the impacts of gully erosion on hydrologic response.

KEYWORDS

Calhoun, critical zone observatory, gully incision, hillslope hydrology, hydrologic modelling

1 | INTRODUCTION

The Southern Piedmont is one of the most severely eroded agricultural areas in the United States (Cowdrey, 1996; Curry, 2010; Richter & Markewitz, 2001). The region lost an average of nearly 20 cm of soil, with severest erosion occurring in the Piedmont of South Carolina (Trimble, 1974). Areas surrounding Calhoun Experimental Forest were identified to have the “poorest Piedmont conditions” (Metz, 1958). Erosion in this region was the combined effect of highly

erodible soilscape, intense rainfall throughout the year and destructive agriculture occupancies during the European settlement in the 18th and 19th century, with last factor being the key driver for shaping the landscape into what it looks like today (Ireland, Sharpe, & Eargle, 1939; Richter, 1987; Richter & Markewitz, 2001; Trimble, 1974). Reduction in fertility caused by excessive erosion led to cultivation-based crops being no longer profitable, leading to the abandonment of land by debt-ridden farmers. Although the old fields are now covered by pine forests, stimulated by warm subtropical

climate of the region, gully erosion still happens occasionally during the hurricane season.

Majority of the investigations on gully erosion in this region has focused on soil loss (Richter, 1987; Trimble, 1974), soil carbon exchange and nutrient cycling (Billings & Richter, 2006; Dialynas, Bastola, Bras, Billings, & Markewitz, 2016; Metz, 1952; Mobley et al., 2015; Richter et al., 2000; Richter & Billings, 2015) and stormwater response (Galang, 2008; Galang, Jackson, Morris, & Markewitz, 2007). How gully erosion impacts the groundwater storage and the root zone soil moisture distribution across the hillslope, and how this impact varies under different gully incision depths remain under-studied. Understanding the impacts of gully erosion on these hydrologic states are important as they directly or indirectly impact groundwater resource availability, runoff generation, streamflow response, hillslope erosion, biogeochemistry in the root zone, and ecohydrological adaptations (Maxwell et al., 2014; Poesen, Nachtergaele, Verstraeten, & Valentin, 2003; USDA, 2015; Wang, Kumar, & Marks, 2013; Zi, Kumar, Kiely, Lewis, & Albertson, 2016). Although there are some studies focused on evaluating the impacts of gully erosion on soil moisture and groundwater storage distribution, they have been executed in the context of montane meadow restoration where gully erosion/channelization occurred in a relatively flat plain within the meadow (Anna & Viers, 2013; Essaid & Hill, 2014; Hammersmark, Rains, & Mount, 2008; Loheide et al., 2009; Loheide & Gorelick, 2007; Lowry & Loheide, 2010; USDA, 2015). In contrast, gullies in the South-eastern Piedmont are surrounded by hillslopes with steepness ranging from 2 to 12% (Galang, 2008). Climatology in the montane meadow landscape is arid or semi-arid (Kottke, Grieser, Beck, Rudolf, & Rubel, 2006) with less than 500 mm annual precipitation, most of which falls in winter as snow. This is also in contrast to the Southern Piedmont which is humid and receives around 1,200 mm of annual precipitation mostly in the form of rain. These differences in physiography and climatology, with added differences in soil structure and vegetation species, are likely to result in differences in the impact of gully erosion on vadose zone soil moisture, groundwater recharge, interaction between vegetation and the subsurface, and streamflow response between the two landscapes.

In this study, we investigated the impact of gully erosion on hydrology of a Piedmont hillslope. To this end, we developed a simplistic, physics-based 2D hydrologic model of a hillslope called

Richards' Equation Python Solver (REPS) that accounts for interception, evapotranspiration, and subsurface flow processes. REPS model was then used to conduct numerical experiments to explore the effects of gully incision on the temporal and spatial variations of groundwater storage and soil moisture. Specifically, the following three questions are addressed in this study:

1. Does the hillslope hydrologic response vary with increasing depth of gully incision?
2. Does the impact of gully incision on soil moisture, groundwater, and transpiration vary in time and space?
3. Is the impact of gully incision on hydrologic responses affected by hydrogeologic properties such as soil hydraulic conductivity, porosity, drainage, bedrock depth, and hillslope steepness?

This article is organized as follows: Section 2 presents the methodology that includes description of the study area and of the developed model. It also describes properties of the 2D hillslopes and model scenarios. Section 3 describes the results from the numerical experiments and discusses the effect of different gully incision depths on hydrologic responses. Section 4 summarizes the findings and presents conclusions and takeaways from this study. Section 5 discusses some additional implications of our findings and limitations of this study.

2 | STUDY AREA AND METHODOLOGY

To answer the questions outlined in Section 1, here we developed a 2D hydrological model, REPS, and performed hydrologic simulations on hillslopes that approximate hydrogeologic and topographic configurations observed at the Calhoun critical zone observatory (CCZO).

2.1 | Study area

The CCZO is located at 34.6°N, 81.7°W in Union County, South Carolina. The observatory is located in the Southern Piedmont region of United States, which has experienced intense gullying (see Figure 1 in

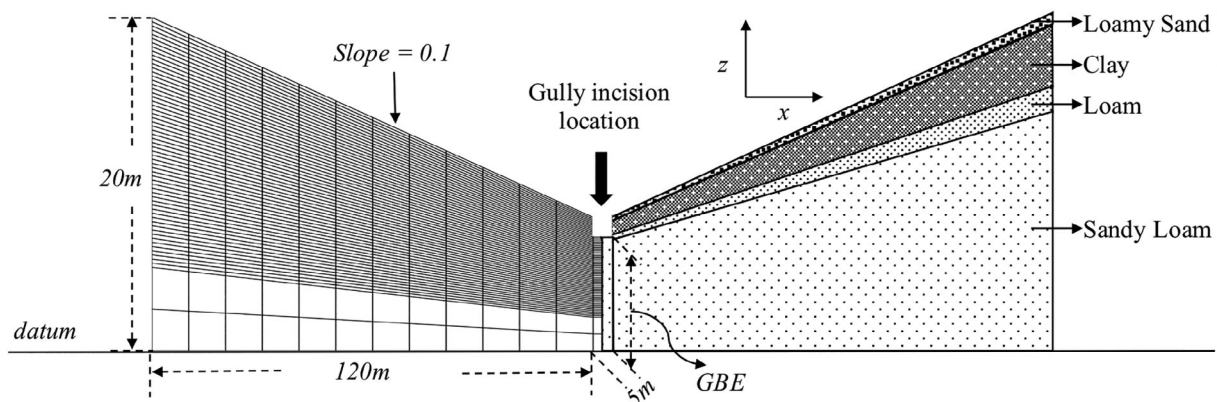


FIGURE 1 Soil profile and dimensions of the representative Calhoun critical zone observatory 2D hillslope. GBE stands for gully bed elevation

Galang, Morris, Markewitz, Jackson, and Carter (2010)) due to combined effects of destructive agriculture occupancies during about 1800 to the 1930s, erodible soils, and intense rainfall regime. The observatory is characterized by a humid temperate climate with long hot summers and short mild winters (Kottek et al., 2006). Based on the data from 2005 to 2014, the average monthly temperature ranges from 5.7°C in January to 28.3°C in July. Annual precipitation ranges from 824 to 1,529 mm, with over half of the precipitation occurring during the hurricane-season (June–November). Soils in the CCZO are typically Ultisols derived from granitic gneiss, and are distinguished by coarse surficial horizons consisting of sandy loams or loamy sands (Richter, 1987). These surficial layers vary in thickness ranging from 0 to around 0.6 m, and overlay a ~2 m thick clay horizon with lower hydraulic conductivity. Below the clay horizons are highly weathered saprolite soils with larger hydraulic conductivity than the overlying clay layer (Richter & Markewitz, 2001). Schematic of the vertical soil profile is shown in the right half of Figure 1. The hillslope considered in this study is part of the transect observed in Clair et al. (2015). The location of the transect is shown in Supporting Information Figure D1. The hillslope is approximated by a trapezoid, with a length of 120 m at the lower boundary, a height of 8 m at the right boundary, and a surface slope of 0.1 (see left hillslope in Figure 1).

REPS is a 2D hydrological model that simulates interception, evapotranspiration including interception loss and transpiration, and subsurface flow processes. Interception is calculated using the Rutter model equation (Rutter & Morton, 1977). The model solves for the 2D pressure head distribution in the subsurface using the variably saturated Richards' equation (Camporese, Paniconi, Putti, & Orlandini, 2010; Kumar, Duffy, & Salvage, 2009; Maxwell & Miller, 2005; Panday & Huyakorn, 2004; Richards, 1931; Therrien, McLaren, Sudicky, & Panday, 2010). Following Wigmosta, Vail, and Lettenmaier (1994), infiltration in the top soil layer is evaluated as the precipitation rate if this rate is less than the unit hydraulic gradient Darcy flux, else the infiltration flux is set equal to the unit gradient Darcy flux. For the latter case, excess precipitation that cannot percolate in the soil contributes to runoff. Because of the steep gradient of the hillslope in the study area, the generated runoff is assumed to flow out of the grid and ponding is not considered. Runoffs from all hillslope grids are pooled together as overland flow (OLF) contribution from the hillslope. Potential evapotranspiration is determined using the Penman equation (Penman, 1948). Actual transpiration from the canopy, T , is determined by Penman–Monteith equation (Monteith, 1964) calculated using the Noilhan–Planton approach (Noilhan & Planton, 1989) as implemented in Zhao, Ji, Kang, Zhang, and Jin (2010). As evaporation from the soil surface underneath the crop cover is closely correlated to transpiration and is often of much smaller magnitude (e.g., Baptista, Bailey, and Meneses (2005) and Xu et al. (2016)), soil surface evaporation is not explicitly considered here. More details about the representation of different processes in the model are presented in the Supporting Information Section A.

Differential equations from each control volume are compiled and solved using a stiff solver based on the Backward Difference Formula method and Newton–Krylov iteration, as implemented in the CVODE solver (Hindmarsh et al., 2005). The solver has been previously used

in several hydrologic, and hydro-biogeochemistry related modelling applications (Bao, Li, Shi, & Duffy, 2017; Chen, Kumar, & McGlynn, 2015; Chen, Kumar, Wang, Winstral, & Marks, 2016; Li & Duffy, 2011; Liu & Kumar, 2016; Park, Wang, & Kumar, 2020; Wang, Kumar, & Link, 2016; Yu, Duffy, Baldwin, & Lin, 2014).

The REPS model was evaluated against experimental and analytical results in both 1D and 2D as described in Supporting Information - Section B. An excellent match was observed between numerical and analytical models.

2.2 | Model setup

The hillslope was discretized into 62 layers in vertical. At the right edge of the modelled hillslope (Figure 1), the discretization resolution in the top 6 m was 0.1 m, while the resolution in the bottom 2 m was 1 m. Fine discretization of the shallow layers was performed to accurately simulate variations in root zone soil moisture and groundwater table (GWT). Vertical resolution at other locations in the hillslope was in proportion to the height of the hillslope at that location. A horizontal discretization resolution of 10 m was chosen for the entire model domain. A thin column representing the subsurface of a gully was included at the right boundary of the hillslope. The vertical discretization of this column was the same as that at the edge of the hillslope, while the horizontal width of the column was set equal to 2.5 m, half of the gully width. The left and bottom boundary of the modelled hillslope was set to no-flow condition. Datum was set at the lower boundary. Total head at the right boundary of the hillslope, above the gully bed, was set equal to its height above datum where the potentiometric head is equal to zero. No-flow boundary condition was applied at the right edge of the gully.

Parameterization of the model domain was performed based on the best on-site data available. Saturated hydraulic conductivity (K_s) for the soil was determined based on a survey at the Calhoun long term soil ecosystem plots (Richter, 2011), where K_s first decreases within the top 1.5 m and then increases downwards, a typical variation that has also been observed in Piedmont saprolite soils at alternative locations (Buol & Weed, 1991). Since K_s in the surveyed data at the site was available only up to 2 m depth, the deeper K_s was approximated based on the vertical K_s profile for the Cecil series soil (one of the most common soil series of the Piedmont) as presented by Buol and Weed (1991). Soil-water drainage characteristics were assigned based on average properties of the identified soil classes (Carsel & Parrish, 1988; Clapp & Hornberger, 1978; Leij, 1996; Nemes, Schaap, Leij, & Wösten, 2001; Tuller & Or, 2004) as presented in Bacon, Bierman, and Rood (2012). Soil class for each soil horizon was first determined by the clay and sand percentages according to the USDA-SCS texture triangle diagram (Brady, 1984). Soil porosity data was determined based on bore data from a 70 m deep well at CCZO, which showed that the porosity first decreases in the top 20 m and then remains unchanged downwards (Steve Holbrook, Virginia Tech., unpublished data). The distribution of soil properties with depth is

Depth (m)	Soil class	α (m^{-1})	n	θ_s ($\text{m}^3 \cdot \text{m}^{-3}$)	θ_r ($\text{m}^3 \cdot \text{m}^{-3}$)	K_s (m/d)
0–0.32	Loamy sand	0.6	1.89	0.558	0.065	0.6216
0.32–1.5	Clay	2.1	1.2	0.5	0.102	0.00672
1.5–2.0	Loam	2.5	1.31	0.558	0.061	0.00864
2.0 >	Sandy loam	2.1	1.61	0.43	0.061	0.06216

TABLE 1 Model parameters for the soil horizons of a representative Calhoun critical zone observatory (CCZO) hillslope

Note: The hillslope is also interchangeably referred to as the heterogeneous hillslope configuration in this study. Definition of parameters are presented in Supporting Information Equations A12 and A13.

listed in Table 1. Soil properties were first defined for the grids at the ridge of the hillslope, then all grids belonging to the same horizontal layer were assigned identical properties. Land cover on the hillslope was assigned the properties of the reference crop as represented in North American Land Data Assimilation System (NLDAS; <https://ldas.gsfc.nasa.gov/nldas/NLDASmapveg.php>). Specific parameter values are listed in Supporting Information Table A1.

Simulations were performed using a 10-year (2005–2014) hourly meteorological forcings dataset at the Calhoun site. The chosen period encompasses a wide range of hydroclimatology with the average precipitation (1,134 mm) close to the long-term average value (1,210 mm for 1895–2016 (Elsner, 2006; NOAA, 2017), and the wettest and driest year annual precipitation falling within the top and bottom 25th percentile for the period 1895–2016. Forcings data for the experiment, including precipitation, temperature, relative humidity, wind velocity, solar radiation, and vapour pressure, were downloaded from the NLDAS, phase 2 (Xia et al., 2012).

2.3 | Design of model scenarios

To understand how gully incision affects the hillslope hydrologic response, a total of 48 REPS model simulations were performed on a range of hillslope configurations with varied hydrogeologic and topographic makeup. For each hillslope configuration, four gully bed elevations (GBEs) or incision depths were considered. Forty-four simulations (11 hillslope configurations \times 4 incision depths) were performed on homogeneous hillslopes (see results presented in Section 3.1) and 4 (1 hillslope configuration \times 4 incision depths) on a heterogeneous hillslope (see results presented in Section 3.2).

Lower GBEs correspond to gully configurations that have undergone more gully incision. The shallowest incision depth was set to 0.5 m (GBE = 7.5 m) below the edge of the hillslope, as 0.5 m is often used as the minimum depth criteria for defining gullies (Imeson & Kwaad, 1980). Other incision depths considered include 1.5 m (GBE = 6.5 m), 2.5 m (GBE = 5.5 m), and 3.5 m (GBE = 4.5 m). The deepest incision depth was set to 3.5 m (GBE = 4.5 m) as gully bed depths as large as 3.0 m have been reported in the Southeastern Piedmont by Galang et al. (2010). The range of incision depths was expected to enable us to understand how the hydrologic response may have changed with progressive incision of gullies in the Southern Piedmont. It is to be noted that the experiment was

not designed to quantify the historical changes in hydrologic response in the CCZO. Such a study would require knowledge of evolving land cover history during the 19th and 20th centuries. For each incision depth configuration, first, a hydrostatic pressure head distribution in the subsurface was assumed. Next, long-term simulation was conducted by repeatedly using the 10-year period forcings until the system reached dynamic equilibrium. The dynamic equilibrium was defined as when the difference in subsurface storage between consecutive 10 years is less than 1 cm (Loheide & Gorelick, 2007). Once the hillslope has reached dynamic equilibrium, simulated states, and fluxes for the next 10-year period was recorded for further analyses. As meteorological forcings and vegetation cover are identical across different simulations, interception loss is expected to be the same as well. Hence, all subsequent discussions concerning the impact on evapotranspiration focus only on the transpiration component.

Simulations performed on the homogeneous hillslope allowed study of the role of hydrogeologic and topographic properties, such as soil conductivity, soil porosity, soil drainage parameters, hillslope steepness, bedrock depth, and soil types, on the impacts of gully incision on hydrologic response. Table 2 lists the parameter values for each of the 11 homogeneous hillslope configurations. The base configuration of the homogeneous hillslope (GBE_{xm}^{*}, shown in grey in Table 2) used the properties of loamy sand, the soil type near the ground surface in the CCZO. Specific properties of this base configuration were modified to further study the influence of topographic and soil properties on the effects of incision on hydrologic responses (see Section 3.1.4). For example, in Table 2, the 'GBE_{xm} Higher K ' hillslope configuration uses 10 times the conductivity of loamy sand soil from the CCZO hillslope, while 'GBE_{xm} Lower K ' uses the conductivity of sandy loam, the other dominant surficial soil in the CCZO hillslope. Cells with '–' in Table 2 indicate that the particular parameter value is the same as that of the base homogeneous configuration. As properties of 'GBE_{xm} Higher θ_s ', 'GBE_{xm} Faster drainage', and 'GBE_{xm} Loamy sand' are identical to that of the base configuration, that is, 'GBE_{xm}^{*}', the 11 unique hillslope configurations are listed in the 14 rows of Table 2. Simulations implemented on the heterogeneous hillslope were designed to provide additional information on the role of horizonation, specifically one that is observed at the CCZO, on gully's impact on hillslope hydrology. In this regard, for a single hillslope configuration, a total of four simulations corresponding to different gully incision depths were conducted. Table 1 lists the properties of soil horizons used to represent the heterogeneous hillslope.

TABLE 2 Model parameters for different configurations of a homogenous hillslope

Homogeneous configurations	K_s (m/d)	θ_s ($\text{m}^3 \cdot \text{m}^{-3}$)	θ_r ($\text{m}^3 \cdot \text{m}^{-3}$)	Surface steepness	α (m^{-1})	n	Soil column height (m)	GBE (m)
GBE _{xm} *	0.6216	0.558	0.065	0.1	0.6	1.89	8	x
GBE _{xm} higher K	6.216	—	—	—	—	—	—	—
GBE _{xm} lower K	0.06216	—	—	—	—	—	—	—
GBE _{xm} higher θ_s	—	0.558	—	—	—	—	—	—
GBE _{xm} lower θ_s	—	0.43	—	—	—	—	—	—
GBE _{xm} faster drainage	—	—	—	—	0.6	1.89	—	—
GBE _{xm} slower drainage	—	—	—	—	2.1	1.61	—	—
GBE _{xm} steeper slope	—	—	—	0.15	—	—	—	—
GBE _{xm} gentler slope	—	—	—	0.05	—	—	—	—
GBE _{xm} deeper bedrock	—	—	—	—	—	—	10	—
GBE _{xm} shallower bedrock	—	—	—	—	—	—	6	—
GBE _{xm} Sandy loam	0.06216	0.43	0.061	—	2.1	1.61	—	—
GBE _{xm} clay	0.00672	0.5	0.102	—	2.1	1.2	—	—
GBE _{xm} loamy sand	0.6216	0.558	0.065	—	0.6	1.89	—	—

Note: x ranges from 4.5 to 7.5 m (at 1 m interval). GBE_{xm}* is the base homogeneous hillslope configuration. It also doubles up as loamy sand, faster drainage, and a higher θ_s hillslope in this study. Specific properties of this base configuration that is, GBE_{xm}* were modified to generate alternative configurations. For example, the 'GBE_{xm} Higher K' hillslope configuration uses 10 times the conductivity of loamy sand soil from the CCZO hillslope while other parameter values are identical (identified by '—') to the base configuration. Definition of parameters are presented in Supporting Information Equations A12 and A13.

3 | RESULTS AND EXPLANATIONS

3.1 | Homogeneous hillslope

3.1.1 | Does the hillslope hydrologic response vary with increasing depth of gully incision?

Simulation on the base homogeneous hillslope (see properties listed in Table 2) showed that with an increase in gully incision, that is, with a decrease in GBE, groundwater flow (GWF) increases while root zone soil moisture and GWT are reduced (Figure 2). If we conceptualize a hillslope as a simple bucket and the gully as an outlet, one may think that the increase of GWF and decrease in GWT with increasing incision, that is, with reduction in outlet elevation, is an obvious result. However, it is to be noted that because of the coupled nature of GWF, vadose zone infiltration, and transpiration, it is likely that increase in GWF triggered by decrease in GBE may change the flux interactions, possibly resulting in extra water entering the hillslope. This possibility was explored using a representative scenario where the GBE was abruptly reduced from 7.5 to 6.5 m. With decrease in the GBE, the GWF gradient increased suddenly, leading to increased GWF (dashed blue line in Figure 3a). This, in turn, triggered a reduction in the GWT (Figure 3b), which caused increased downward flow from the top soil and lateral flow from the ridge of the hillslope. The redistribution of moisture resulted in reduction in root zone soil saturation (Figure 3c), which led to increased infiltration (Supporting Information Figure C1) and reduced transpiration (Figure 3d and Figure C1). With time, the GWF gradually reduced and infiltration

gradually increased until the long-term infiltration rate (incoming flux to the hillslope) was roughly equal to the GWF plus the transpiration from root zone (outgoing flux from the hillslope). For the hillslope under consideration, this transition from one dynamic equilibrium (corresponding to GBE_{7.5 m}) to another (corresponding to GBE_{6.5 m}) was nearly complete by the end of the second year (Figure 3), that is, when the dashed blue line almost coincided with the red line. Hydrologic fluxes such as infiltration (INFIL), transpiration (T), groundwater recharge, and GWF and OLF contributions to gully, and changes in total water storage (ΔS) and groundwater (ΔGW) are shown in Table 3. For the scenario depicting abrupt reduction in GBE, hereafter called GBE_{7.5 to 6.5 m}, the total gain of water in the hillslope during the first 2 years was 0.110 m, which included increment in infiltration by 0.095 (=1.590–1.495) m and reduction in transpiration by 0.015 (=1.234–1.249) m (differences in the flux magnitudes correspond to the values between scenarios GBE_{7.5 m to 6.5 m} and GBE_{7.5 m} in Table 3). The total loss of water during this period, from increased GWF, was 0.342 m (=0.939–0.597). Net water loss from the hillslope, that is, ΔS , was 0.232 (=–0.583 to [–0.351]) m, with 0.390 (=–0.819 to [–0.429]) m loss in the groundwater storage (ΔGW) and 0.158 m gain in the vadose zone. Notably, even though the vadose zone gained water as GBE decreases, the average saturation level in the vadose zone reduced because of a larger increase in total vadose zone volume due to the decline in GWT. These results confirm our earlier assertion that although on the first impression it appears that the impact of gully incision on GWT is obvious, this is not really so. Incision alters a multitude of fluxes and hydrologic states, and assessment of impacts should appropriately consider coupled interactions between them.

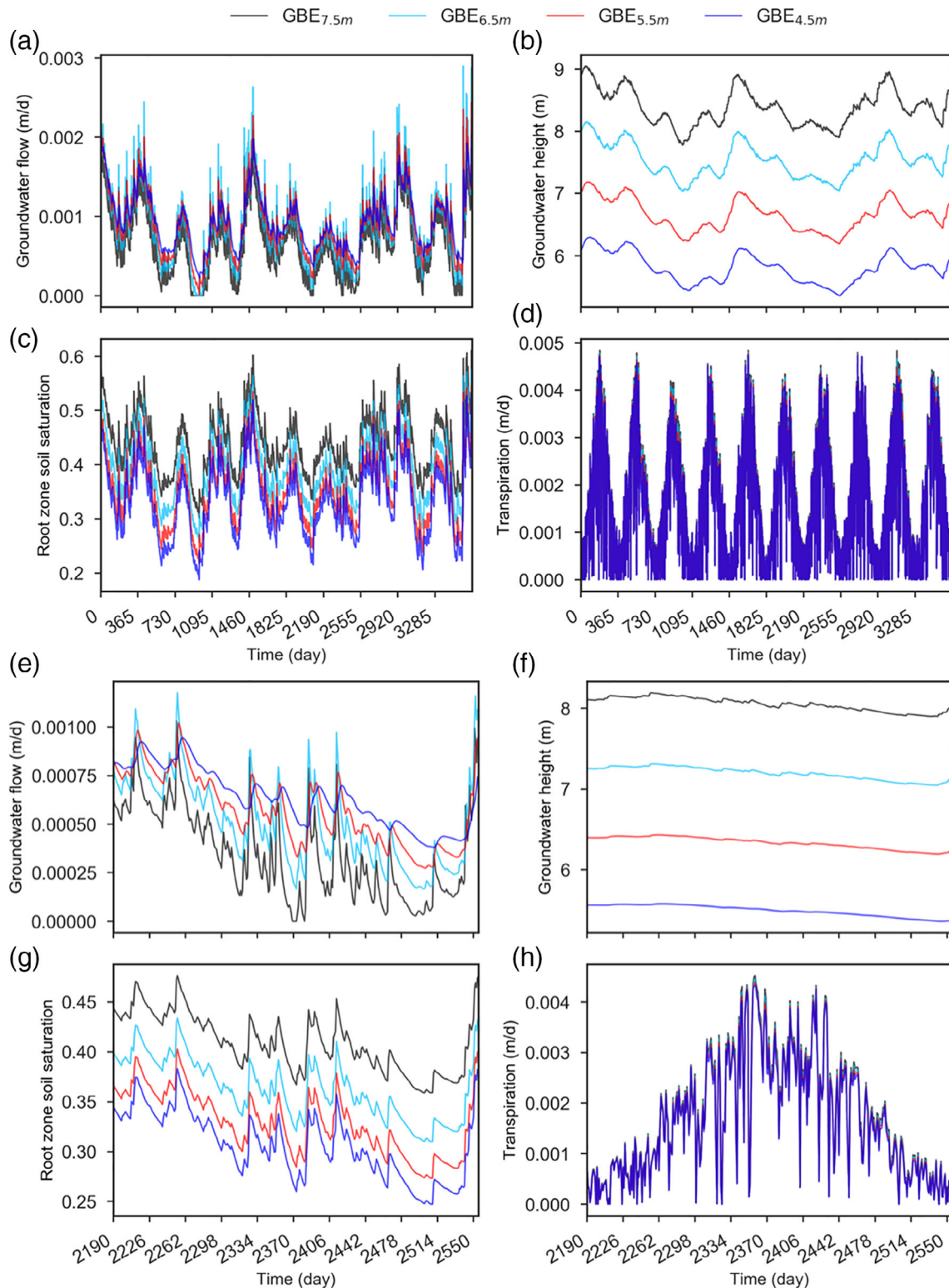


FIGURE 2 A 10 year (a–d) and an average year (e–h) snapshot of daily variations of groundwater flow, groundwater table, root zone soil saturation, and transpiration, for the base homogeneous hillslope (see properties listed in Table 2). Results are shown for four gully incision depths or gully bed elevations (GBEs)

The reduction in GWT and the drying of soil profile due to gully incision are consistent with observations in semi-arid Tigray highlands of Ethiopia by Moeyersons (2000). However, the increase in GWF

with incision is in contrast to the results reported for Bacao complex in Brazil (Lima, Bacellar, & Drumond, 2018), where the removal of the soil profile with spatial proliferation of gullies reduced the effective

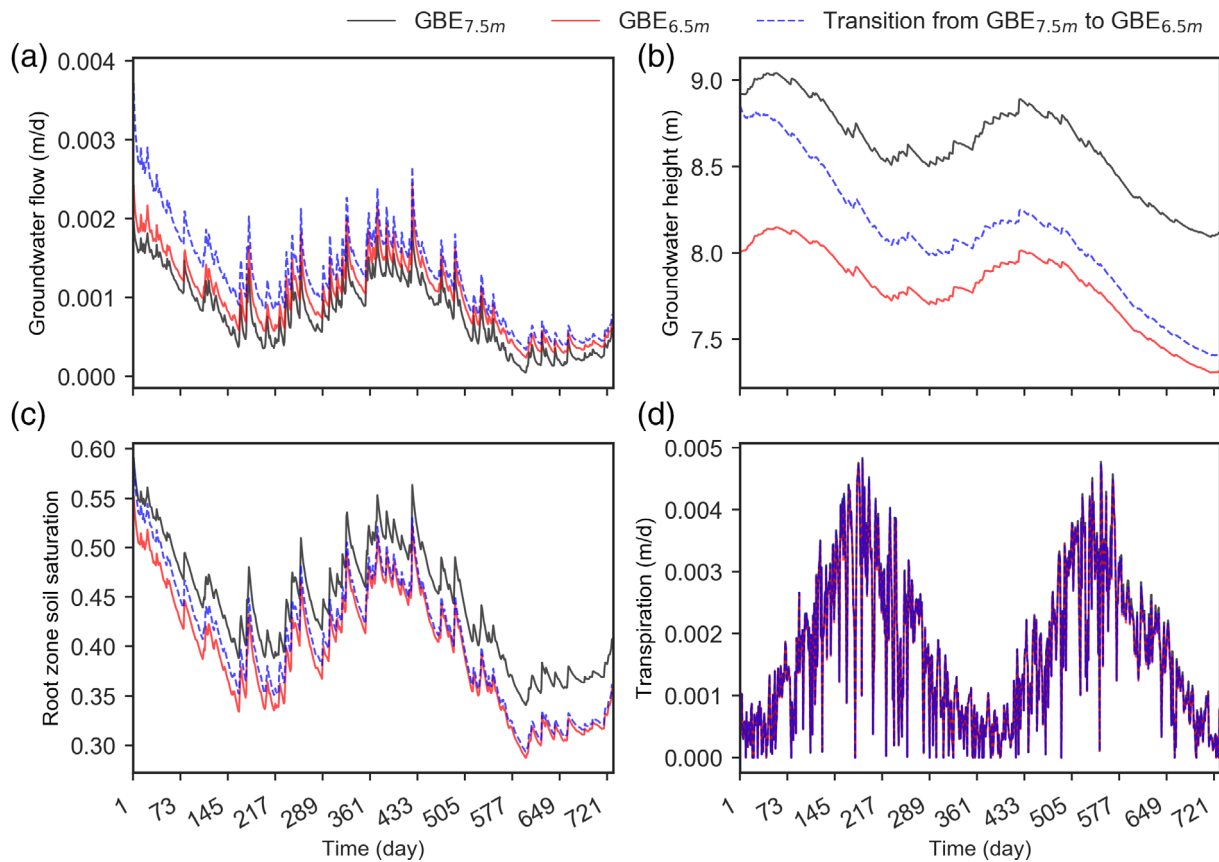


FIGURE 3 Daily variations of groundwater flow, groundwater table, root zone soil saturation, and transpiration during the first 2 years of transition from gully bed elevation (GBE) of 7.5 m that is, GBE_{7.5m} to GBE_{6.5m} for the base homogeneous hillslope configuration (see properties listed in Table 2). Also shown are the corresponding variations for the hillslope with GBE_{7.5m} and GBE_{6.5m}

TABLE 3 Hydrologic states and fluxes (in metre) for the base homogeneous hillslope configuration (see properties listed in TABLE 2) during the transition from gully bed elevation (GBE) = 7.5 m to GBE = 6.5 m

Scenarios	Fluxes and storage during the first 2 years						
	OLF	GWF	T	Infiltration	ΔS	ΔGW	Recharge
GBE _{7.5m}	0.120	0.597	1.249	1.495	-0.351	-0.429	0.169
GBE _{6.5m}	0.020	0.745	1.224	1.595	-0.375	-0.368	0.377
GBE _{7.5to6.5m}	0.025	0.939	1.234	1.590	-0.583	-0.819	0.120
Scenarios	Average value of fluxes and storage during the 10-year simulation period						
	OLF	GWF	T	Infiltration	ΔS	ΔGW	Recharge
GBE _{7.5m}	0.058	0.246	0.629	0.874	0.022	0.000	0.246
GBE _{6.5m}	0.004	0.313	0.616	0.929	0.020	-0.001	0.313
GBE _{7.5to6.5m}	0.005	0.337	0.618	0.928	-0.006	-0.051	0.287

Abbreviations: GW, groundwater; GWF, groundwater flow; OLF, overland flow; S, storage; T, transpiration.

recharge area for the underlying aquifer resulting in reduction of base-flow. Notably, the result presented here only considers the effects of increased incision and does not account for the impacts of spatial proliferation of gullies. Another result that is in disagreement with earlier findings is the reduction of GWT with increased incision, which was reported to increase in wet years at a montane meadow site (Essaid & Hill, 2014; Loheide & Gorelick, 2007; USDA, 2015). The difference is largely due to contrasting recharge mechanisms in the two systems. In

the considered Piedmont hillslope, the groundwater recharge is mostly from incoming precipitation and infiltration. However, in the meadow, the mountain block recharge also contributes to dynamics of groundwater storage. Depending on the mountain block recharge magnitude, and the relative hydraulic conductivity of the mountain block and the meadow, GWT in meadow systems may increase even when GBE reduces (Loheide et al., 2009). Similarly, reduction of runoff or OLF with lowering of GBE is also in contradiction with findings in

Hammersmark et al. (2008) and Ohara et al. (2014). This is partly because OLF in Piedmont hillslope is largely due to saturation of the soil above the clay horizon, whereas groundwater saturation excess is the dominant mechanism for runoff generation in a meadow. During wet and flood periods, reduction in GBE can lead to increase in GWT in meadows, thus causing large runoff generation as well.

Figure 2b shows that the average GWT height in the hillslope was higher than the GBE. This is attributed to the positive recharge to the groundwater through precipitation events. A negligible recharge to the groundwater, otherwise, would have resulted in GWT to be at the same elevation as the GBE. Another important observation from Figure 2 is that the reduction in GWT with gully incision was generally smaller than the reduction in GBE. For each additional 1 m reduction in GBE from 7.5 to 4.5 m, the average GWT reduced by around 0.86 m. This was because of a persistent increase in the average recharge rate to

groundwater as GBE reduced. An example of increase in recharge with reduction in GBE is shown in Table 3. The increase in recharge is attributable to a reduction in root zone soil saturation and an increase in infiltration rate as incision increases. Notably, with increasing incision, the magnitude of decrease of OLF and increase of GWF diminishes, while the reduction in transpiration remains the same. For example, as GBE changed from 7.5 to 4.5 m, the change in overland and GWF diminished from 0.054 m and 0.067 m respectively for the transition from $GBE_{7.5m}$ to $GBE_{6.5m}$, to 0.002 and 0.015 m respectively for $GBE_{6.5m}$ to $GBE_{5.5m}$, and 0 and 0.013 m respectively for $GBE_{5.5m}$ to $GBE_{4.5m}$ (see hillslope configuration GBE_{xm}^* in Table 4). However, transpiration changed by 0.013 m ($=0.629-0.616$), 0.013 m ($=0.616-0.603$), and 0.013 m ($=0.603-0.590$) as GBE decreased from 7.5 to 4.5 m, in steps of 1 m, respectively. The results indicate that change in overland and GWF per unit incision depth is greatest as gullies begin their incision. Notably,

TABLE 4 Average annual flux out of the hillslope for a range of homogenous and heterogeneous CCZO hillslope configurations (HCs)

HC	x	OLF	GWF	T	HC	x	OLF	GWF	T
GBE_{xm}^*	7.5	0.058	0.246	0.629	GBE_{xm} CCZO	7.5	0.181	0.056	0.667
	6.5	0.004	0.313	0.616		6.5	0.120	0.120	0.667
	5.5	0.002	0.328	0.603		5.5	0.074	0.167	0.667
	4.5	0.002	0.341	0.590		4.5	0.044	0.199	0.666
GBE_{xm} higher K	7.5	0.031	0.330	0.570	GBE_{xm} lower K	7.5	0.274	0.013	0.611
	6.5	0.000	0.387	0.548		6.5	0.253	0.039	0.605
	5.5	0.000	0.411	0.526		5.5	0.247	0.055	0.596
	4.5	0.000	0.438	0.502		4.5	0.247	0.070	0.583
GBE_{xm} Steeper slope	7.5	0.039	0.301	0.570	GBE_{xm} gentler slope	7.5	0.111	0.136	0.661
	6.5	0.002	0.349	0.562		6.5	0.012	0.246	0.652
	5.5	0.002	0.357	0.554		5.5	0.002	0.273	0.638
	4.5	0.002	0.365	0.546		4.5	0.002	0.296	0.619
GBE_{xm} higher θ_s	7.5	0.058	0.246	0.606	GBE_{xm} lower θ_s	7.5	0.061	0.246	0.602
	6.5	0.004	0.313	0.595		6.5	0.005	0.319	0.591
	5.5	0.002	0.328	0.583		5.5	0.002	0.336	0.577
	4.5	0.002	0.341	0.570		4.5	0.002	0.351	0.563
GBE_{xm} deeper bedrock	7.5	0.057	0.249	0.603	GBE_{xm} shallower bedrock	7.5	0.061	0.237	0.611
	6.5	0.004	0.317	0.592		6.5	0.005	0.307	0.600
	5.5	0.002	0.332	0.579		5.5	0.002	0.322	0.587
	4.5	0.002	0.346	0.566		4.5	0.002	0.336	0.576
GBE_{xm} Sandy loam	7.5	0.258	0.034	0.604	GBE_{xm} clay	7.5	0.724	0.000	0.209
	6.5	0.247	0.063	0.586		6.5	0.724	0.001	0.209
	5.5	0.247	0.074	0.577		5.5	0.724	0.001	0.208
	4.5	0.247	0.076	0.576		4.5	0.724	0.003	0.208
GBE_{xm} faster drainage	7.5	0.058	0.246	0.606	GBE_{xm} slower drainage	7.5	0.006	0.274	0.634
	6.5	0.004	0.313	0.595		6.5	0.002	0.285	0.626
	5.5	0.002	0.328	0.583		5.5	0.002	0.294	0.618
	4.5	0.002	0.341	0.570		4.5	0.002	0.294	0.617

Note: Properties of the heterogeneous configuration, that is, GBE_{xm} CCZO, are presented in Table 1, while that of the homogeneous configurations (all configurations other than GBE_{xm} CCZO are homogeneous) are presented in Table 2. x ranges from 4.5 to 7.5 m (at 1 m interval) and indicates the 4 gully incision depths or gully bed elevations (GBEs).

Abbreviations: CCZO, Calhoun critical zone observatory; GWF, groundwater flow; OLF, overland flow; T, transpiration.

the change in transpiration per unit incision depth remains almost the same. This indicates that the influence on hydrologic fluxes with further gully incision varies with hillslope fluxes.

3.1.2 | Does gully incision alter the temporality of hillslope hydrologic response?

Transpiration estimated on the base homogeneous hillslope (see properties listed in Table 2) showed a strong seasonality with its magnitude being the largest during summer and smallest during winter. Since precipitation is almost evenly distributed over the year, high transpiration rates in summer led to depletion of both root zone moisture and GWT. Because of larger recharge in winter compared with summer, GWT was higher in winter, leading to larger GWF as well (Figure 4a,e). Variation of aforementioned fluxes and states over the year followed a similar temporal pattern for other GBEs as well.

To study the impacts of gully incision on the temporal variation of fluxes and states, we evaluated the differences between two consecutive GBEs (as shown in Figure 4b–d,f–h). Positive values in Figure 4b–d indicate an increase and negative values indicate a decrease in fluxes and states with increasing gully incision. In accordance with the results in Section 3.1.1, negative values in ΔT indicate that transpiration was reduced when gully bed was lower. The plot also shows that the reduction in transpiration was largest during summer and smallest during winter. This was primarily because of the seasonality of potential transpiration. Because of the large reduction in transpiration in summer, the reduction in root zone soil moisture in summer was larger. Overall, OLF also reduced (negative values in ΔOLF in Figure 4b) due to lower root zone moisture which resulted in increased infiltration under $GBE_{6.5m}$ (see hillslope configuration GBE_{xm}^* in Table 4). Notably, the reduction in OLF and transpiration showed similar temporal variations as the increment in GWF, that is, the summation of black and red bars was very similar to the cyan bar (Figure 4b). In other words, the increase in infiltration (/reduction in OLF) and reduction in transpiration resulted in more recharge to the GWT, thus contributing to an increase in GWF. Since this increment in recharge was largest in summer, reduction in GWT during summer was the smallest (as shown in Figure 4f). Consequently, GWF experienced the largest increase in summer as well (as shown in Figure 4b). In agreement with the results in Section 3.1.1, with further reduction in GBE (Figure 4c,d), OLF continued to reduce and GWF continued to increase, and this reduction/increment magnitude became smaller as the gully incision deepened (Figure 4b–d). Notably, the increase in GWF with gully incision did not happen across all seasons. For example, GWF reduced during winter with reduction in GBE from 6.5 to 4.5 m. This is in part due to the influence of smaller reduction in GWT in summer with incision, which imparts a time-lagged influence on GWF. The RZS and GWT also reduced for lower GBE. However, reduction in GWT did not show a significant difference under different GBEs. Reduction in RZS was largest when GBE changed from 7.5 to 6.5 m and gradually became smaller as GBE reduced further (Figure 4f–h).

3.1.3 | Does gully incision alter the hillslope hydrologic response spatially?

Long-term average GWT height, root zone saturation, top soil saturation, and transpiration rate at different locations (from ridge to toe) of the base homogeneous hillslope (see properties listed in Table 2) under varied gully incisions are shown by solid lines in Figure 5. Shaded region in the plot indicates the [5, 95] percentile of variation in the respective variable over the 10 years. The average groundwater height exhibited a curved profile, with lower height near the toe of the hillslope. The difference in GWT height between head and toe of the hillslope was larger for deeper incision depths, that is, lower GBEs, to support larger GWF. Given that the average inclination angle of GWT was much smaller than the hillslope surface, GWT in areas near the toe of the hillslope were shallower and hence were wetter due to capillarity (Figure 5b). It is to be noted that this moisture distribution pattern is opposite to that in the incised meadow (see figure 14 in Loheide and Gorelick (2007) for more details) with near level hillslope and small GWT inclination angle. Because of higher soil moisture near the toe of hillslope, both average top soil saturation and root zone soil saturation were also larger. However, spatial variation of average transpiration did not always follow the spatial variation of average root zone saturation (Figure 5d). Although root zone soil saturation monotonically increased from ridge to toe of the hillslope, with rate of increase being higher near the toe of the hillslope, transpiration first increased similarly but then reached a plateau. The plateau is reached when the soil moisture is mostly above the S_{cr} value (see Supporting Information Equation A6). As GBE reduced, the starting point of the plateau moved towards the toe of the hillslope due to reduction in root zone saturation, which resulted in less hillslope area with root zone moisture being above S_{cr} . As the GBE became lower, both soil moisture and GWT reduced across the hillslope, with the greatest reductions occurring at the toe of the hillslope and much smaller changes at the ridge of the hillslope. For transpiration, the largest reductions occurred near the starting point of the plateau for $GBE = 7.5$ m. These results suggest that impact of gully incision on soil moisture and GWT is most pronounced near the gully, and gradually vanishes as moving away from the incised location. However, the impact on evapotranspiration is most pronounced at some distance from the toe of the hillslope. Notably, vegetations at this location are likely to be more susceptible to increased gully incision.

Variation of groundwater height during the 10 years was greatest at the ridge of the hillslope and smallest at the toe of the hillslope (Figure 5a). Since GWT was shallow near the toe of the hillslope during both wet and dry periods, root zone soil saturation (Figure 5b) remained high and did not vary as much as that near the ridge of the hillslope. In contrast, the magnitude of variation in transpiration expressed varied trends (Figure 5d). For shallow gully depths (e.g., $GBE = 7.5$ m), the variation is largest near the channel and smaller farther from the channel. For locations with high water availability (e.g., toe of hillslope), the transpiration rate is high in summer and low in winter (limited by energy), however, at locations with low water availability (e.g., ridge of hillslope), the transpiration rate in summer is moisture limited and in winter it is energy limited thus resulting in a much smaller variation range.

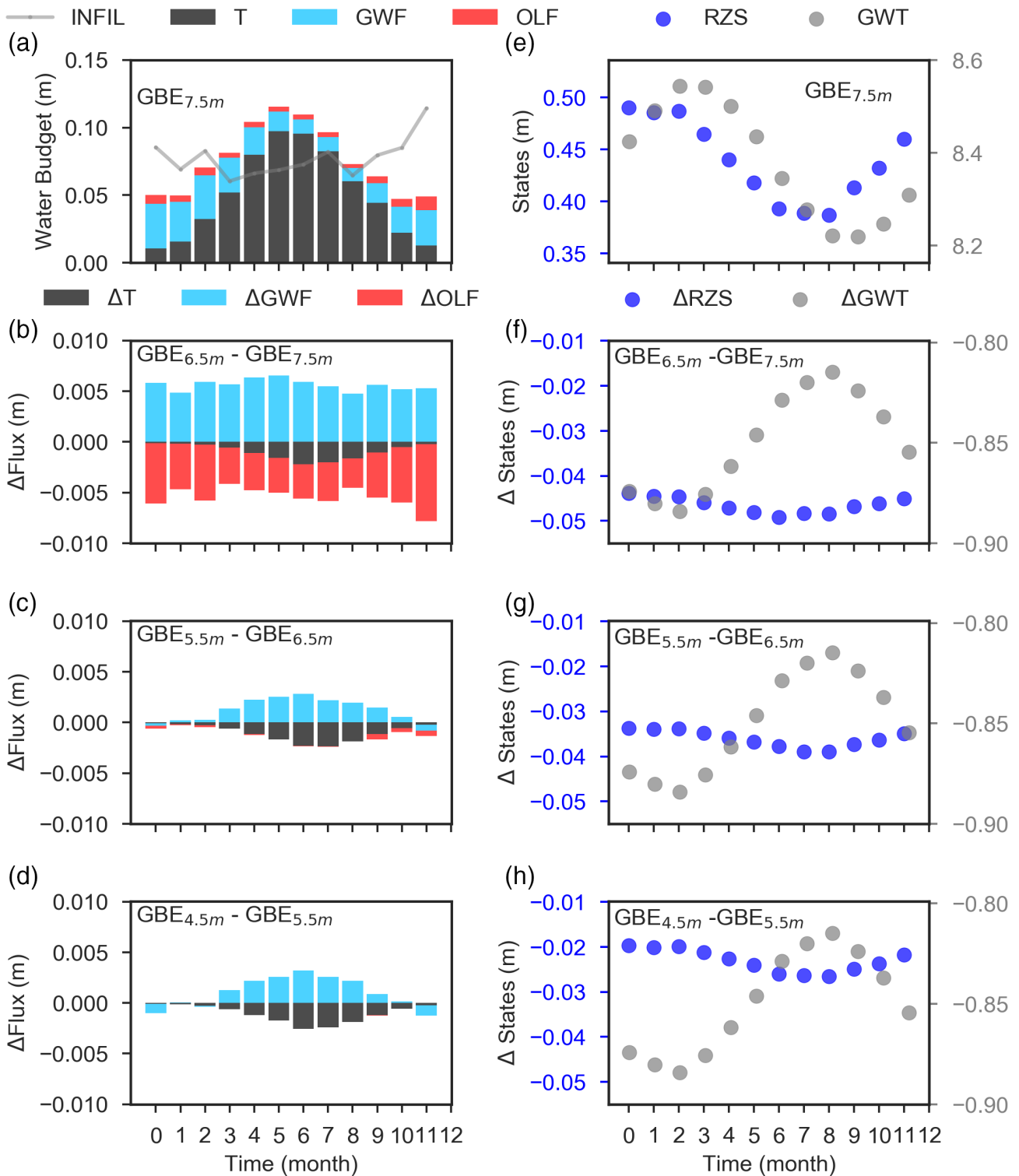


FIGURE 4 Hydrologic states and fluxes for the base homogeneous hillslope configuration (see properties listed in Table 2) during the 10-year simulation period. (a) Monthly average infiltration (INFIL), transpiration (T), groundwater flow (GWF), and overland flow (OLF); (e) Monthly average groundwater table (GWT) and root zone saturation (RZS). Difference of hydrologic fluxes and states between scenarios with gully bed elevation (GBE) equal to 7.5 m that is, GBE_{7.5m} and GBE_{6.5m} are shown in (b) and (f), between GBE_{6.5m} and GBE_{5.5m} are shown in (c) and (g), and between GBE_{5.5m} and GBE_{4.5m} are shown in (d) and (h), respectively

However, for deeper gully depths (e.g., GBE = 4.5 m), the magnitude of variation in transpiration first increased and then subsequently plateaued from head to toe of the hillslope. This was because variations in

the transpiration was not only controlled by variations in the average moisture content in the root zone, but also by vertical distribution of moisture in the root zone, meteorological variations, and root

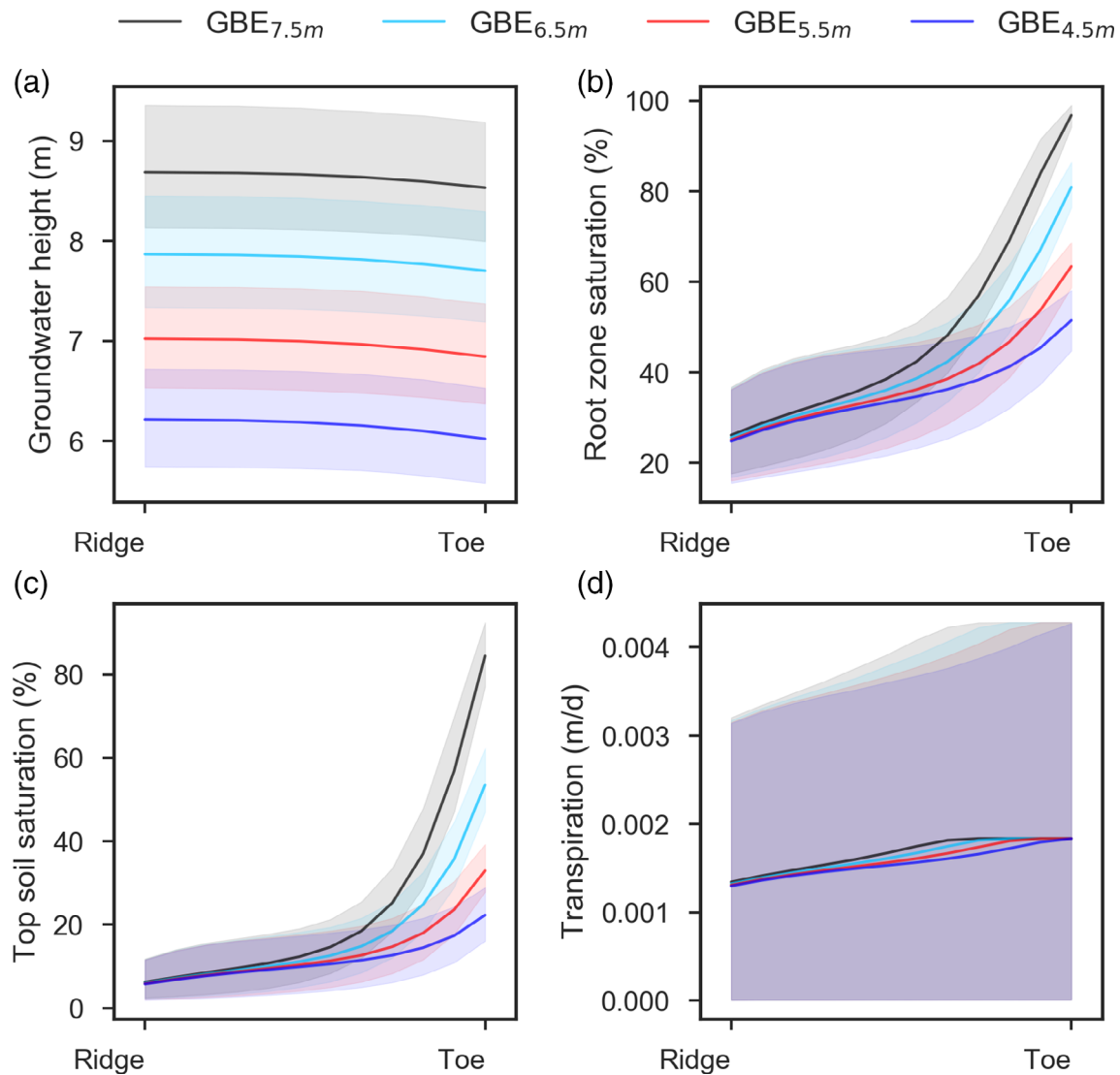


FIGURE 5 Long-term average (the solid lines) and variations (the shaded areas, indicating 5–95 percentile range of variations) of groundwater height, root zone saturation, top soil saturation, and transpiration, for the base homogeneous hillslope (see properties listed in Table 2). Results are shown for four gully incision depths or gully bed elevations (GBEs). x-Axis in the above plots extends from ridge to toe of the hillslope that is depicted in the left-hand side of Figure 1

distribution. Notably, variation in root zone soil saturation near toe of the hillslope increased with incision. This was because of deepening of the groundwater, which resulted in variation of soil moisture being dominantly determined by incoming precipitation rather than capillary rise. The variation in transpiration at the toe of hillslope reduced as GBE lowered. The cause for this was limited water availability in the root zone under lower GBE.

3.1.4 | Does the impact of gully incision on hydrologic responses vary with hydrogeologic properties?

Impacts of gully erosion under different soil conductivities, soil porosities, soil drainage parameters, hillslope steepness, soil types, and

bedrock depths were explored by considering a range of homogeneous hillslope configurations (see properties in Table 2). As illustrated in Figure 6, the hydrologic responses for the considered range of properties follow variations that are similar to those presented for the base homogeneous hillslope configuration in Sections 3.1.1–3.1.3. These include: (a) reduction in the GWT, root zone soil moisture, top soil saturation, OLF, and transpiration with deeper incision or lower GBE; (b) increase in the GWF for lower GBE; (c) higher reduction in transpiration and larger increment in GWF during summer, while a smaller reduction in GWT during summer; (d) smaller changes in fluxes and states per unit increase in incision once the gully was deep to begin with; and (e) relatively muted impact on transpiration and soil moisture with increasing distance from the incised channel. However, the magnitude of increase or decrease of different states or fluxes varied with hydrogeologic properties.

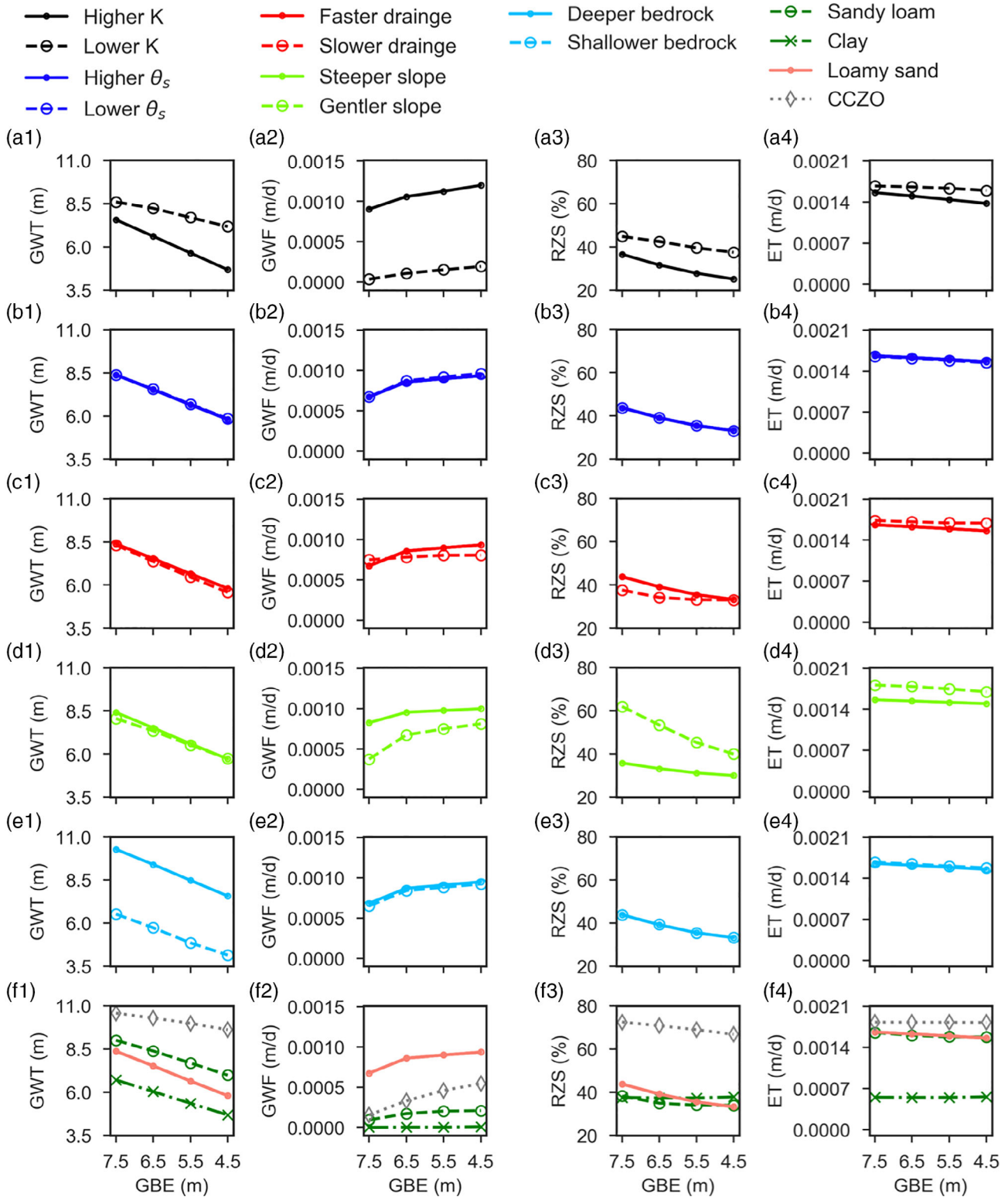


FIGURE 6 Long-term average groundwater table height (GWT), groundwater flow (GWF), root zone saturation (RZS [%]) and transpiration (T) under different incision depths or gully bed elevations (GBEs) for a range of hillslope configurations (HCs). HCs are identified by their defining characteristics in the legend. For example, 'Higher K' denotes 'GBE_{xm} Higher K' in Table 2. Panels in a column show impacts of gullying on a given hydrologic variable (GWT, GWF, RZS, and T). Properties of the heterogeneous configuration, that is, the Calhoun critical zone observatory (CCZO), are presented in Table 1, while the homogeneous configuration properties (all configurations other than CCZO are homogeneous) are presented in Table 2

Impact of hillslope hydraulic conductivity

Hillslope with higher soil conductivity had lower GWT, RZS, and ET, but higher GWF under $GBE_{7.5m}$ (as shown in Figure 6a1–a4). This was because higher conductivity hillslopes flushed groundwater at relatively high rates (Figure 6,a2), resulting in a lower GWT and consequently lower RZS and ET (Figure 6,a3,a4). As GBE reduced, hillslopes with higher soil conductivity experienced a larger reduction in GWT due to larger increases in GWF from the hillslope in comparison to the low conductivity hillslopes (see GBE_{xm}^* , GBE_{xm} Higher K, and GBE_{xm} Lower K in Table 4, and Figure 6a1–a4). For example, the reduction in GWT in high conductivity hillslope almost followed the reduction in GBE, that is, 3 m reduction in GWT as GBE reduced by 3 m. In contrast, GWT reduction in low conductivity hillslope was much less, that is, only 0.4 m reduction in GWT as GBE reduced by 3 m. A larger rate of reduction in GWT also led to higher rate of decrease in RZS and ET for the high conductivity hillslope.

In summary, with a reduction in GBE, a hillslope with higher hydraulic conductivity experienced a larger change in fluxes and states, indicating that hydrology of such hillslopes are relatively vulnerable to gully incision.

Impact of soil porosity

Although soil porosity impacted the temporal variability of moisture response and the total moisture volume, for the range of porosities considered here, its impact on the long-term average GWT, GWF, RZS, and ET rate was relatively small (Figure 6b1–b4).

Impact of soil drainage parameters

Hillslopes with higher drainage rates (drainage characteristic shown in Supporting Information Figure C2) generally experienced larger rate of decrease in RZS and ET, and a slightly smaller rate of decrease in GWT with reduction in GBEs (Figure 6c1–c4). With the lowering of GBE, GWT height was reduced, which in turn created a moisture deficit in the vadose zone. For more rapid drainage, a similar moisture deficit led to more drainage, resulting in a larger reduction in RZS and ET. However, this also led to increased recharge to groundwater, which reduced the rate of decrease of GWT with reduction in GBE.

Impact of surface slope

A hillslope with steeper surface slope yielded higher GWT and GWF out of the hillslope, but lower root zone soil saturation and transpiration rate, provided all other configurations remain the same (see GBE_{xm}^* , GBE_{xm} Steeper slope, and GBE_{xm} Gentler slope in Table 4, and Figure 6d1–d4). As the distance between gully bed and the surface of the hillslope was larger for steeper hillslopes, for the same GWT height, the soil saturation in the vadose zone was smaller. This resulted in smaller root zone soil saturation and transpiration rate, and larger infiltration rate and groundwater recharge. Consequently, OLF amount in steeper hillslopes was smaller while the GWT was higher.

As GBE is reduced, steeper hillslopes experienced larger reduction in GWT but smaller increases in GWF and smaller decreases in RZS and ET (see GBE_{xm}^* , GBE_{xm} Steeper slope, and GBE_{xm} Gentler slope in Table 4, and Figure 6d1–d4). This was because, between steep and

gentle slopes, moisture deficit created by lowering of GBE created a smaller increase in the rate of groundwater recharge in steeper hillslopes due to lower soil saturation in the vadose zone. This also resulted in smaller decrease of RZS and ET with GBE for steeper hillslopes.

Impact of bedrock depth

Hillslopes with different bedrock depth showed small differences in hydrologic response (Figure 6e2–e4). Although the GWT height appeared to be notably different, most of it was just due to the difference in the bedrock depth. With deeper bedrock, the lateral flow to the aquifer below the gully increases. This translated to lower GWT for deeper bedrock case, if the difference in bedrock depth, which was 4 m here, was subtracted from it. Lower GWT for deeper bedrock case resulted in lower RZS and ET as well.

Impact of soil types

Comparison of hydrologic responses was performed for three of the four most contrasting soil types found in the CCZO hillslope (Table 1). Sandy loam and loamy sand hillslopes showed differences (Figure 6f1–f4) that were similar to that between hillslopes with higher and lower conductivity soils (Figure 6a1–a4). This was not surprising, as sandy loams indeed have a lower conductivity than loamy sands (Table 1). However, the response of clay hillslope was very different. Despite having lower conductivity and drainage rate than sandy loam, GWT in clay hillslope was found to be much smaller than in the loamy sand hillslope (Figure 6f1). Also, the rate of reduction of GWT with GBE was also higher than that in sandy loam hillslope. This seemed unreasonable at first, given that lower conductivity soils are expected to have higher average GWT and a lower rate of reduction in GWT with GBE (see Figure 6a1–a4). The unusual response of clay hillslope is attributable to its significantly low conductivity, which is much smaller than the conductivities considered in Figure 6a1–a4. The low conductivity of clays allowed very small amount of infiltration, most of which was lost through evapotranspiration. This resulted in negligible recharge to groundwater. As a result, the average GWT height equilibrated to the GBE, which translated to lower average GWT and a faster rate of reduction in GWT with reduction in GBE w.r.t. the sandy loam case.

The above six comparison experiments showed that soil hydraulic conductivity strongly influenced hillslope responses under gully incision. Steepness of the hillslope was also found to have an effect on hillslope responses with steeper hillslopes showing larger reduction in GWT with lowering of GBE. In contrast, soil drainage parameters had relatively modest impacts. Influences of soil porosity and bedrock depth were almost negligible.

3.2 | Heterogeneous CCZO hillslope

Simulations were also conducted on a heterogeneous CCZO hillslope with a representative soil horization as indicated in Figure 1 and with properties as defined in Table 1. The average runoff ratio for the simulation period was 0.24, which is close to the runoff ratio of 0.23

in watershed 4 of the Calhoun CZO during the historical period for which data exists (Wang, Shen, & Shahnaz, 2018). Similar runoff value of 0.22 was also observed by Hendrickson (1963) in another watershed in the Southern Piedmont. Notably, the runoff ratio falls within the reported range of 0.16–0.56 in the southeastern U.S. watersheds (Chang, Johnson, Hinkley, & Jung, 2014). These comparisons indicate that the long-term water budget partitioning for the considered hillslope is realistic. Model results also show development of two distinct saturation layers near the ridge. In contrast, only one GWT was apparent near the toe of the hillslope. Notably, this is consistent with observation results in watershed 4 of CCZO (Mallard, McGlynn, & Richter, 2017; see Supporting Information Figure C3), and is another proof that the representation of water partitioning in the subsurface is reasonable and representative of the landscape. Formation of an additional perched saturation layer or shallow GWT at the ridge site was due to ponding above the low permeability clay horizon after precipitation events. This happened even while the GWT was deeper. However, near the toe of the hillslope, which also acts as convergence zone of the GWF, GWT is shallow enough to be above the clay layer most of the time.

Results showed that with increasing gully incision depth, GWF out of the hillslope is enhanced while the OLF is diminished (see GBE_{xm} CCZO in Table 4), which is consistent with the trend shown in homogeneous hillslopes. However, transpiration is identical for all incision depths. Even though the soil at the ground surface is loamy sand, the hydrology of CCZO hillslope seems to be relatively less susceptible to gully incision. For instance, reduction in GWT height with lowering of GBE was smaller than for a homogeneous hillslope composed completely of either sandy loam, clay or loamy sand soil (Figure 6f1). In addition, the difference in average annual transpiration as GBE was lowered from 7.5 to 4.5 m, was much smaller than both the sandy loam and loamy sand hillslopes (Figure 6f4). Notably, the actual transpiration rate and the RZS for CCZO hillslope was much higher than other hillslope configurations considered in Figures 6f3–f4, even though its root zone lies within the loamy sand or clay soil horizons. This is because infiltration occurring in the top loamy sand layer gets trapped above the clay layer resulting in high RZS and transpiration rate. Lower rate of recharge through the clay layer also ends up in lowering the GWT in this hillslope with respect to the homogeneous sandy loam hillslope.

Patterns of monthly variation in hydrologic variables (Figure 7a) for the shallowest incision case ($GBE_{7.5m}$) were similar to that shown in the homogeneous case (Figure 4a), with transpiration being larger in summer and smaller in winter, GWT being lower in summer and higher in winter, and OLF and GWF being larger in winter and smaller in summer. The impact on these variables for different GBEs (Figure 7b–d,f–h) also showed similar (positive or negative change) trend as that in the homogeneous scenarios. Notably, the change magnitude of hydrologic states and fluxes as GBE reduced from 7.5 to 6.5 m were much smaller than that shown in the base homogeneous case (Figures 7b and Figure 4b). With further reductions in GBE, the magnitude of flux change reduced slower than that shown in the homogeneous base case (Figures 7c,d) and Figure 4c,d). This again indicates that the heterogeneous CCZO hillslope is much less susceptible to changes in the boundary conditions

with respect to the homogeneous loamy sand hillslope. Similar to the base homogeneous case, changes in GWT and RZS were again largest in winter and smallest in summer.

Spatial variations of different fluxes and states over the 10-year period (see Figure 8) exhibited similar behaviour as that shown in the base homogeneous hillslope, where the effect of gully incision was the largest at the toe of hillslope and diminished towards the ridge. However, the effect of gully incision at the toe of the CCZO hillslope was much smaller than the base hillslope. For example, GWT at the toe of the heterogeneous CCZO hillslope only reduced by an average of 0.32 m as GBE reduced 1 m, while the reduction in base homogeneous hillslope was around 0.86 m. Similarly, root zone saturation, top soil saturation and transpiration all showed much smaller change than in the base hillslope. Notably, magnitude of variations in these variables was much larger than that in the base hillslope. In addition, unlike the overall monotonic trend in magnitude of variations from the toe to the ridge shown in the homogeneous hillslope, variation magnitude in the CCZO hillslope was largest in-between the toe and ridge of the hillslope. This is due to interaction between perched saturation above the clay layer and its interaction with the root zone which extends to different depths in the clay layer.

The results showed that the response of groundwater storage and root zone soil moisture in the heterogeneous CCZO hillslope under gully incision was overall in agreement with that in the homogeneous hillslopes. However, hydrology in the upper part of the heterogeneous CCZO hillslope was relatively resilient to gully incision due to the existence of a low conductivity clay layer which served as a 'barrier' and effectively divided the CCZO hillslope into two storage elements. As a result, hydrology in upper storage element was only mildly affected by reduction in GBE.

4 | SUMMARY AND CONCLUSIONS

This study evaluated the impact of gully incision on hillslope hydrologic responses, including GWT, root zone soil moisture, transpiration, overland, and GWF out of the hillslope. Our results showed that with increasing gully incision (decreasing GBE), GWF out of the hillslope were enhanced, while GWT, root zone moisture, transpiration, and runoff were all diminished. The study highlights that through gully erosion, the landscape not only loses soil but may also lose a significant amount of water from the subsurface. Furthermore, the impacts of gully incision extend far beyond the GWT, with both the root zone soil moisture and transpiration getting affected as well. Given the coupled influence of soil moisture on atmospheric boundary layer dynamics (Findell & Eltahir, 2003) and vegetation mortality (Liu et al., 2017), this may have consequences on ecological adaptations and overall vegetation productivity too. As groundwater recharge also increased with gully incision in most cases, it points to the potential for using gully trenching methods to increase groundwater recharge and baseflow (Somers et al., 2018).

The change in hillslope fluxes and states such as GWT, root zone moisture, overland, and GWF, in response to a reduction in GBE, was

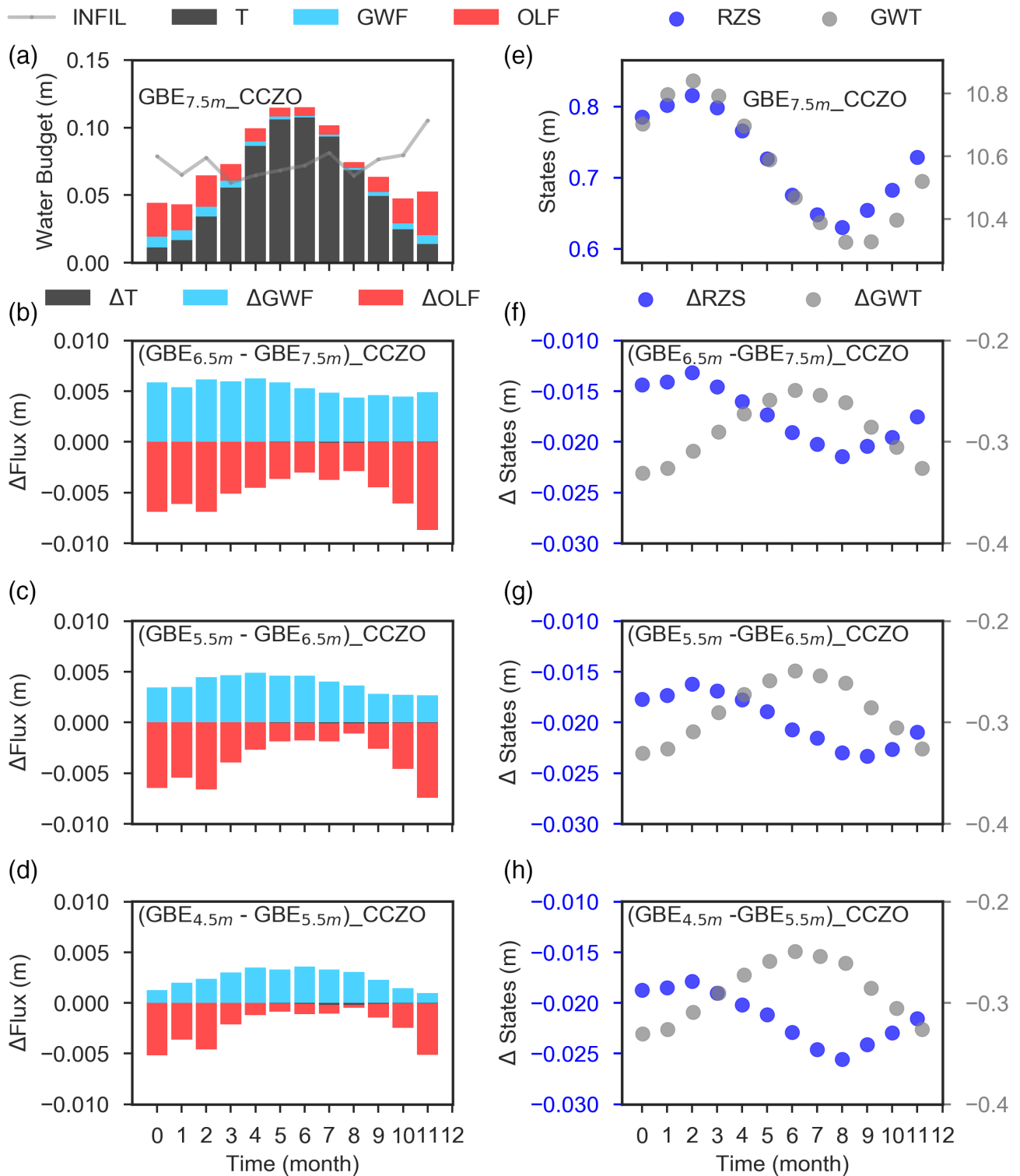


FIGURE 7 Hydrologic states and fluxes for the heterogeneous hillslope configuration (see properties listed in Table 1) during the 10-year simulation period. (a) Monthly average infiltration (INFIL), transpiration (T), groundwater flow (GWF), and overland flow (OLF); (e) Monthly average groundwater table (GWT) and root zone saturation (RZS). Difference of hydrologic fluxes and states between gully bed elevation (GBE) equal to 7.5 m that is, GBE_{7.5m} and GBE_{6.5m} are shown in (b) and (f), between GBE_{6.5m} and GBE_{5.5m} are shown in (c) and (g), and between GBE_{5.5m} and GBE_{4.5m} are shown in (d) and (h), respectively

found to be larger in shallow gullies. The impacts generally diminished as the gully bed became deeper. These points to the possibility of reduced effectiveness of trenching methods for gullies that are

already deep. It also means that schemes implemented to prevent gully and its consequent hydrologic impacts should prioritize shallower, often younger, gullies. Spatially, the impact of gully incision

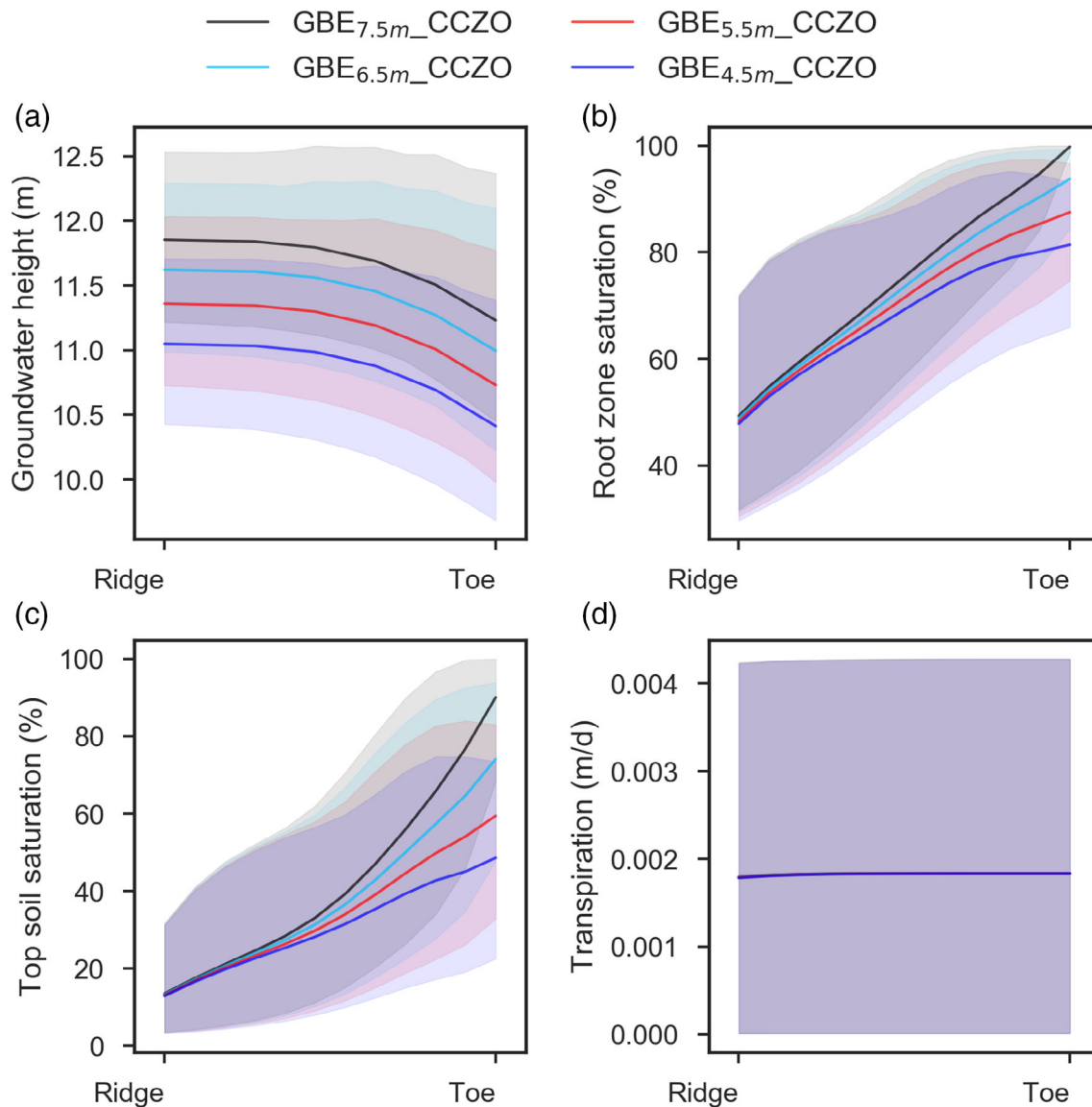


FIGURE 8 Long-term average (the solid lines) and variations (the shaded areas, indicating 5–95 percentile range of variations) of groundwater height, root zone saturation, top soil saturation, and evapotranspiration in the representative CCZO hillslope (also referred to as the heterogeneous hillslope configuration). x-Axis in the above plots extends from ridge to toe of the hillslope that is depicted in the left-hand side of Figure 1

on GWT and root zone moisture was greatest at locations near the incised channel or toe of the hillslope. However, the impact on vegetation transpiration was largest at some distance from the toe of the hillslope, close to where the root zone soil moisture was above the critical value most of the time for shallow gully depths. Given the spatially varied impact of gully incision on root zone soil moisture and transpiration, impact assessment studies should use sampling strategies that span the hillslope transect. Temporally, reduction in transpiration and increase in groundwater recharge due to gully incision was greatest in summer. As a result, the reduction of GWT due to gully incision was also the smallest in summer. The result highlights the need to obtain observations of hydrologic states and/or fluxes through all seasons to more accurately assess the impacts of gully incision on hillslope hydrology.

Overall, the hydrologic impacts of gully erosion were found to be dependent on a range of hydrogeological properties. The extent of the impact was, however, most strongly influenced by hillslope soil hydraulic conductivity and surface steepness, and much less by soil porosity, drainage parameters, and bedrock depth. For a hillslope with higher hydraulic conductivity, the decrease in GWT, root zone soil saturation, and transpiration with gully incision were much more intense. Between steeper and milder hillslopes, root zone soil saturation and transpiration showed a smaller decline with gully incision in steeper hillslopes. These results indicate that schemes implemented to prevent gully incision and its consequent hydrologic impacts should prioritize flatter hillslopes, especially those with relatively high subsurface hydraulic conductivity.

The extent of impact of gully incision on hydrologic response for a heterogeneous hillslope was very different with respect to a

homogeneous surrogate made of dominant soil properties. For example, for the hillslope with representative horizonation from the Calhoun CZO, it was found that clay horizons serve as a 'barrier' that divides the hillslope into two storage elements thus effectively moderating the effects of gully incision on root zone hydrology. In the absence of the clay layer, the Piedmont would have likely suffered larger change in root zone hydrology and transpiration due to gulying. The result underscores the need for explicitly represent existing horizonations in the subsurface for assessment of the impacts of gulying on hillslope hydrology. Using a homogenous equivalent of the subsurface as an alternative may yield significantly different estimates both in terms of extent and trend (i.e., an increase or a decrease).

5 | DISCUSSION

The study details the influence of topographic and hydrogeologic makeup of hillslopes on hydrologic response to gulying. This information may be used to guide the development of simplistic conceptual models to assess the relative susceptibility of a hydrologic system to increased gully incision. For example, the impact on GWT can be summarized using the following conceptual model

$$\Delta\text{GWT} = f(\Delta\text{GBE}; K, \text{BRD}, S_h) \quad (1)$$

where ΔGWT is the decrease in GWT due to gulying, ΔGBE is the incision extent, K is equivalent saturated hydraulic conductivity of the hillslope, BRD is the bedrock depth at the toe of the hillslope, and S_h is slope of the hillslope. $f(v; p_1, p_2, \dots, p_n)$ is a functional relation between ΔGWT and variable v (ΔGBE in this case) subject to parameters p_i . The model captures a directly proportional decrease in ΔGWT with gully incision intensity (ΔGBE). Furthermore, the accentuating impact of higher hydraulic conductivity, bedrock depth, and the slope is captured as well. As more intense gully incision, that is larger ΔGBE , is expected in settings with high rainfall erosivity, large contributing area, and erodible gully beds with steep bed slopes (Istanbulluoglu, Tarboton, Pack, & Luce, 2003; Tucker & Bras, 1998), such locations are likely to experience larger GWT loss due to gully incision. So, Equation (1) can be rewritten as

$$\Delta\text{GWT} = f(R.A.S_r; K, \text{BRD}, S_h) \quad (2)$$

where R is the rainfall erosivity, A is contributing area of a gully location, and S_r is slope of the stream bed. Similar conceptualizations relating the influence of landscape property on gully incision and its consequent impacts on root zone soil moisture, GWF, and transpiration may be developed for other fluxes and states as well, based on the variations shown in Figure 6.

The scope of this study is limited to understanding the effects of gulying on the hydrology of a Piedmont hillslope that is static in time. As erosion in gullies occurs at a much higher rate than on the hillslopes, the static representation of hillslope is reasonable. The study also does not consider concomitant changes in land use/land cover and soil

properties that may occur during the time when incision happens. Furthermore, feedback on hillslope hydrologic properties due to changes in gully incision is ignored as well. Despite these limitations, the study facilitates understanding of (a) the possible impacts of gulying on hillslope hydrology; (b) how the impacts may vary with intensity of gulying, and topographic and hydrogeological property of the hillslope; and (c) how the impacts may vary in space and time. Further confidence in the conclusions could be gained by validation of simulated responses in controlled settings such as those performed in eXperimental Landscape Evolution Facility (Singh, Reinhardt, & Fofoula-Georgiou, 2015) and Landscape Evolution Observatory (Pangle et al., 2015). Future studies interested in quantifying the actual historical changes in hydrologic response in the CCZO during the 19th and 20th century should duly consider the evolving geomorphology of the landscape and the land cover history of the region, their effects on gully incision, and the coupled feedbacks. Such an effort will likely require development and implementation of an integrated, spatially explicit, hydrologic-landscape evolution-vegetation dynamics modelling framework.

ACKNOWLEDGEMENT

This study was partially funded by National Science Foundation grants EAR-1331846, EAR-1920425, and EAR-1856054.

DATA AVAILABILITY STATEMENT

The data that support the findings of this study are available from the corresponding author upon reasonable request.

ORCID

Xing Chen  <https://orcid.org/0000-0002-8391-3010>

Mukesh Kumar  <https://orcid.org/0000-0001-7114-9978>

REFERENCES

- Anna, F.-H., & Viers, J. H. (2013). *Sierra Nevada Meadow Hydrology Assessment. Final Project Report to the USDA Forest Service Pacific Southwest Region (USFS PSW)*. Davis, CA: University of California.
- Bacon, A. R., Bierman, P. R., & Rood, D. H. (2012). Coupling meteoric ^{10}Be with pedogenic losses of ^9Be to improve soil residence time estimates on an ancient North American interfluvium. *Geology*, 40(9), 847–850.
- Bao, C., Li, L., Shi, Y., & Duffy, C. (2017). Understanding watershed hydrogeochemistry: 1. Development of RT-flux-PIHM. *Water Resources Research*, 53(3), 2328–2345. <https://doi.org/10.1002/2016wr018934>
- Baptista, F., Bailey, B., & Meneses, J. (2005). Measuring and modelling transpiration versus evapotranspiration of a tomato crop grown on soil in a Mediterranean greenhouse. *Acta Horticulturae*, 691(1), 313. <https://doi.org/10.17660/ActaHortic.2005.691.36>
- Billings, S., & Richter, D. D. (2006). Changes in stable isotopic signatures of soil nitrogen and carbon during 40 years of forest development. *Oecologia*, 148(2), 325–333.
- Brady, N. C. (1984). *The nature and properties of soils*, 9. London: Macmillan Publishing Company.
- Buol, S., & Weed, S. (1991). Saprolite-soil transformations in the Piedmont and Mountains of North Carolina. *Geoderma*, 51(1–4), 15–28.
- Camporese, M., Paniconi, C., Putti, M., & Orlandini, S. (2010). Surface-subsurface flow modeling with path-based runoff routing, boundary condition-based coupling, and assimilation of multisource observation data. *Water Resources Research*, 46(2), 1–22. <https://doi.org/10.1029/2008WR007536>

- Carsel, R. F., & Parrish, R. S. (1988). Developing joint probability distributions of soil water retention characteristics. *Water Resources Research*, 24(5), 755–769.
- Chang, H., Johnson, G., Hinkley, T., & Jung, I.-W. (2014). Spatial analysis of annual runoff ratios and their variability across the contiguous US. *Journal of Hydrology*, 511, 387–402. <https://doi.org/10.1016/j.jhydrol.2014.01.066>
- Chen, X., Kumar, M., & McGlynn, B. L. (2015). Variations in streamflow response to large hurricane-season storms in a southeastern US watershed. *Journal of Hydrometeorology*, 16(1), 55–69.
- Chen, X., Kumar, M., Wang, R., Winstral, A., & Marks, D. (2016). Assessment of the timing of daily peak streamflow during the melt season in a snow-dominated watershed. *Journal of Hydrometeorology*, 17(1), 2225–2244. <https://doi.org/10.1175/JHM-D-15-0152.1>
- Clair, J. S., Moon, S., Holbrook, W., Perron, J., Riebe, C., Martel, S., ... Singha, K. (2015). Geophysical imaging reveals topographic stress control of bedrock weathering. *Science*, 350(6260), 534–538.
- Clapp, R. B., & Hornberger, G. M. (1978). Empirical equations for some soil hydraulic properties. *Water Resources Research*, 14(4), 601–604.
- Cowdrey, A. E. (1996). *This land, this south: An environmental history*, Lexington, KY: University Press of Kentucky.
- Curry, A. E. (2010). *Emancipation and erosion: Tenant farming, sharecropping, and soil erosion on the South Carolina Piedmont, 1860–1925* (Masters theses). Millersville University of Pennsylvania.
- Dialynas, Y. G., Bastola, S., Bras, R. L., Billings, S. A., & Markewitz, D. (2016). Topographic variability and the influence of soil erosion on the carbon cycle. *Global Biogeochemical Cycles*, 30(5), 644–660. <https://doi.org/10.1002/2015GB005302>
- Elsner, J. B. (2006). Evidence in support of the climate change–Atlantic hurricane hypothesis. *Geophysical Research Letters*, 33(16), L16705. <https://doi.org/10.1029/2006GL026869>
- Essaid, H. I., & Hill, B. R. (2014). Watershed-scale modeling of streamflow change in incised montane meadows. *Water Resources Research*, 50(3), 2657–2678.
- Findell, K. L., & Eltahir, E. A. (2003). Atmospheric controls on soil moisture–boundary layer interactions. Part I: Framework development. *Journal of Hydrometeorology*, 4(3), 552–569.
- Galang, M. A. (2008). *Prescribed burning effects on gully hydrology, erosion, and soil phosphorus pools in the Piedmont region of South Carolina* (Unpublished doctoral dissertation), The University of Georgia.
- Galang, M. A., Jackson, C. R., Morris, L. A., Markewitz, D., & Carter, E. (2007). *Hydrologic behavior of gullies in the South Carolina piedmont* (p. 633). Paper presented at the Proceedings of the 2007 Georgia Water Resources Conference, March 27–29, 2007, University of Georgia, Athens, GA.
- Galang, M. A., Morris, L. A., Markewitz, D., Jackson, C. R., & Carter, E. A. (2010). Prescribed burning effects on the hydrologic behavior of gullies in the South Carolina Piedmont. *Forest Ecology and Management*, 259(10), 1959–1970. <https://doi.org/10.1016/j.foreco.2010.02.007>
- Hammersmark, C. T., Rains, M. C., & Mount, J. F. (2008). Quantifying the hydrological effects of stream restoration in a montane meadow, northern California, USA. *River Research and Applications*, 24(6), 735–753.
- Hendrickson, B. H. (1963). *Runoff and erosion control studies on Cecil soil in the southern Piedmont* (Vol. 1281). Washington DC: US Dept. of Agriculture.
- Hindmarsh, A. C., Brown, P. N., Grant, K. E., Lee, S. L., Serban, R., Shumaker, D. E., & Woodward, C. S. (2005). SUNDIALS: Suite of nonlinear and differential/algebraic equation solvers. *ACM Transactions on Mathematical Software (TOMS)*, 31(3), 363–396. <https://doi.org/10.1145/1089014.1089020>
- Imeson, A., & Kwaad, F. (1980). Gully types and gully prediction. *Geografisch Tijdschrift*, 14, 430–441.
- Ireland, H. A., Sharpe, C. F. S., & Eargle, D. (1939). *Principles of gully erosion in the Piedmont of South Carolina*. Washington DC: US Dept. of Agriculture.
- Istanbulluoglu, E., Tarboton, D. G., Pack, R. T., & Luce, C. (2003). A sediment transport model for incision of gullies on steep topography. *Water Resources Research*, 39(4), 1103–1117.
- Kottek, M., Grieser, J., Beck, C., Rudolf, B., & Rubel, F. (2006). World map of the Köppen-Geiger climate classification updated. *Meteorologische Zeitschrift*, 15(3), 259–263. <https://doi.org/10.1127/0941-2948/2006/0130>
- Kumar, M., Duffy, C. J., & Salvage, K. M. (2009). A second-order accurate, finite volume-based, integrated hydrologic modeling (FIHM) framework for simulation of surface and subsurface flow. *Vadose Zone Journal*, 8(4), 873–890.
- Leij, F. J. (1996). *The UNSODA unsaturated soil hydraulic database: user's manual* (Vol. 96). Cincinnati, OH: National Risk Management Research Laboratory, Office of Research and Development, US Environmental Protection Agency.
- Li, S., & Duffy, C. J. (2011). Fully coupled approach to modeling shallow water flow, sediment transport, and bed evolution in rivers. *Water Resources Research*, 47(3), 1–20.
- Lima, P. G. d., Bacellar, L. d. A. P., & Drumond, F. N. (2018). Quantification by numerical simulation of the impact of gullies on the water budget of a basement area, southeastern Brazil. *Hydrological Sciences Journal*, 63(12), 1804–1816.
- Liu, Y., & Kumar, M. (2016). Role of meteorological controls on interannual variations in wet-period characteristics of wetlands. *Water Resources Research*, 52, 5056–5074. <https://doi.org/10.1002/2015wr018493>
- Liu, Y., Parolari, A. J., Kumar, M., Huang, C.-W., Katul, G. G., & Porporato, A. (2017). Increasing atmospheric humidity and CO₂ concentration alleviate forest mortality risk. *Proceedings of the National Academy of Sciences of the United States of America*, 114(37), 9918–9923.
- Loheide, S. P., Deitchman, R. S., Cooper, D. J., Wolf, E. C., Hammersmark, C. T., & Lundquist, J. D. (2009). A framework for understanding the hydroecology of impacted wet meadows in the Sierra Nevada and Cascade ranges, California, USA. *Hydrogeology Journal*, 17(1), 229–246. <https://doi.org/10.1007/s10040-008-0380-4>
- Loheide, S. P., & Gorelick, S. M. (2007). Riparian hydroecology: A coupled model of the observed interactions between groundwater flow and meadow vegetation patterning. *Water Resources Research*, 43(7), 1–16.
- Lowry, C. S., & Loheide, S. P. (2010). Groundwater-dependent vegetation: Quantifying the groundwater subsidy. *Water Resources Research*, 46(6), 1–8.
- Mallard, J., McGlynn, B., & Richter Jr, D. (2017). *Terrain and subsurface influences on runoff generation in a steep, deep, highly weathered system*. Paper presented at the AGU Fall Meeting Abstracts.
- Maxwell, R. M., & Miller, N. L. (2005). Development of a coupled land surface and groundwater model. *Journal of Hydrometeorology*, 6(3), 233–247. <https://doi.org/10.1175/JHM422.1>
- Maxwell, R. M., Putti, M., Meyerhoff, S., Delfs, J.-O., Ferguson, I. M., Ivanov, V., ... Sulis, M. (2014). Surface-subsurface model intercomparison: A first set of benchmark results to diagnose integrated hydrology and feedbacks. *Water Resources Research*, 50(2), 1531–1549. <https://doi.org/10.1002/2013WR013725>
- Metz, L. J. (1952). Weight and nitrogen and calcium content of the annual litter fall of forests in the South Carolina Piedmont. *Soil Science Society of America Journal*, 16(1), 38–41.
- Metz, L. J. (1958). *The Calhoun experimental forest*, 1–24. Asheville, NC: USDA Forest Service. <https://doi.org/10.5962/bhl.title.115583>
- Moblely, M. L., Lajtha, K., Kramer, M. G., Bacon, A. R., Heine, P. R., & Richter, D. D. (2015). Surficial gains and subsoil losses of soil carbon and nitrogen during secondary forest development. *Global Change Biology*, 21(2), 986–996.
- Moeyersons, J. (2000). Desertification and man in Africa. *Bulletin des Séances*, 46(2), 151–170.
- Monteith, J. (1964). *Evaporation and environment*. Paper presented at the Symposia of the society for experimental biology.

- Nemes, A., Schaap, M., Leij, F., & Wösten, J. (2001). Description of the unsaturated soil hydraulic database UNSODA version 2.0. *Journal of Hydrology*, 251(3), 151–162.
- NOAA. (2017). National Centers for Environmental Information (National Oceanic and Atmospheric Administration). Retrieved from https://www.ncdc.noaa.gov/cag/time-series/us/38/0/pcp/ytd/12/1895-2017?base_prd=true&firstbaseyear=1901&lastbaseyear=2000
- Noilhan, J., & Planton, S. (1989). A simple parameterization of land surface processes for meteorological models. *Monthly Weather Review*, 117(3), 536–549. [https://doi.org/10.1175/1520-0493\(1989\)117<0536:Aspols>2.0.Co;2](https://doi.org/10.1175/1520-0493(1989)117<0536:Aspols>2.0.Co;2)
- Ohara, N., Kavvas, M., Chen, Z., Liang, L., Anderson, M., Wilcox, J., & Mink, L. (2014). Modelling atmospheric and hydrologic processes for assessment of meadow restoration impact on flow and sediment in a sparsely gauged California watershed. *Hydrological Processes*, 28(7), 3053–3066.
- Panday, S., & Huyakorn, P. S. (2004). A fully coupled physically-based spatially-distributed model for evaluating surface/subsurface flow. *Advances in Water Resources*, 27(4), 361–382. <https://doi.org/10.1016/j.advwatres.2004.02.016>
- Pangle, L. A., DeLong, S. B., Abramson, N., Adams, J., Barron-Gafford, G. A., Breshears, D. D., ... Dontsova, K. (2015). The landscape evolution observatory: A large-scale controllable infrastructure to study coupled earth-surface processes. *Geomorphology*, 244, 190–203.
- Park, J., Wang, D., & Kumar, M. (2020). Spatial and temporal variations in the groundwater contributing areas of inland wetlands. *Hydrological Processes*, 34(5), 1117–1130. <https://doi.org/10.1002/hyp.13652>
- Penman, H. L. (1948). Natural Evaporation from Open Water, Bare Soil and Grass. *Proceedings of the Royal Society of London*, 193, 120–145. <https://doi.org/10.1098/rspa.1948.0037>
- Poesen, J., Nachtergaele, J., Verstraeten, G., & Valentin, C. (2003). Gully erosion and environmental change: Importance and research needs. *Catena*, 50(2–4), 91–133. [https://doi.org/10.1016/s0341-8162\(02\)00143-1](https://doi.org/10.1016/s0341-8162(02)00143-1)
- Richards, L. A. (1931). Capillary conduction of liquids through porous mediums. *Journal of Applied Physics*, 1(5), 318–333.
- Richter, R. B. (1987). Soil erosion and degradation in the southern Piedmont of the USA. *Land Transformation in Agriculture*, (pp. 407–428). London: Wiley.
- Richter, D. D. (2011). CZO dataset: Calhoun long-term soil experiment - soil survey (2011) - hydraulic conductivity. Retrieved from <http://criticalzone.org/calhoun/data/dataset/4106/>
- Richter, D. D., & Billings, S. A. (2015). 'One physical system': Tansley's ecosystem as Earth's critical zone. *New Phytologist*, 206(3), 900–912.
- Richter, D. D., & Markewitz, D. (2001). *Understanding soil change: Soil sustainability over millennia, centuries, and decades*. New York, NY: Cambridge University Press.
- Richter, D. D., Markewitz, D., Heine, P. R., Jin, V., Raikes, J., Tian, K., & Wells, C. G. (2000). Legacies of agriculture and forest regrowth in the nitrogen of old-field soils. *Forest Ecology and Management*, 138(1), 233–248.
- Rutter, A., & Morton, A. (1977). A predictive model of rainfall interception in forests. III. Sensitivity of the model to stand parameters and meteorological variables. *Journal of Applied Ecology*, 14, 567–588.
- Singh, A., Reinhardt, L., & Fofoula-Georgiou, E. (2015). Landscape reorganization under changing climatic forcing: Results from an experimental landscape. *Water Resources Research*, 51(6), 4320–4337.
- Somers, L. D., McKenzie, J. M., Zipper, S. C., Mark, B. G., Lagos, P., & Baraer, M. (2018). Does hillslope trenching enhance groundwater recharge and baseflow in the Peruvian Andes? *Hydrological Processes*, 32(3), 318–331. <https://doi.org/10.1002/hyp.11423>
- Therrien, R., McLaren, R., Sudicky, E., & Panday, S. (2010). *HydroGeoSphere: A three-dimensional numerical model describing fully-integrated subsurface and surface flow and solute transport*. Waterloo, ON: Groundwater Simulations Group, University of Waterloo.
- Trimble, S. W. (1974). *Man-induced soil erosion on the southern Piedmont—1700–1970*. Ankeny, IA: Soil Conserv. Soc. Am.
- Tucker, G. E., & Bras, R. L. (1998). Hillslope processes, drainage density, and landscape morphology. *Water Resources Research*, 34(10), 2751–2764.
- Tuller, M., & Or, D. (2004). Retention of water in soil and the soil water characteristic curve. *Encyclopedia of Soils in the Environment*, 4, 278–289.
- USDA. (2015). *Effects of meadow erosion and restoration on groundwater storage and baseflow in national forests in the Sierra Nevada, California*.
- Wang, J., Shen, Y., & Shahnaz, S. (2018). *Calhoun experimental forest, SC - streamflow/discharge, precipitation (1949–1962)*. Retrieved from <http://criticalzone.org/calhoun/data/dataset/4680/>
- Wang, R., Kumar, M., & Link, T. E. (2016). Potential trends in snowmelt-generated peak streamflows in a warming climate. *Geophysical Research Letters*, 43(10), 5052–5059.
- Wang, R., Kumar, M., & Marks, D. (2013). Anomalous trend in soil evaporation in a semi-arid, snow-dominated watershed. *Advances in Water Resources*, 57, 32–40. <https://doi.org/10.1016/j.advwatres.2013.03.004>
- Wigmosta, M. S., Vail, L. W., & Lettenmaier, D. P. (1994). A distributed hydrology-vegetation model for complex terrain. *Water Resources Research*, 30(6), 1665–1679. <https://doi.org/10.1029/94WR00436>
- Xia, Y., Mitchell, K., Ek, M., Sheffield, J., Cosgrove, B., Wood, E., ... Mocko, D. (2012). Continental-scale water and energy flux analysis and validation for the North American land data assimilation system project phase 2 (NLDAS-2): 1. Intercomparison and application of model products. *Journal of Geophysical Research. Atmospheres*, 117(3), 1–27. <https://doi.org/10.1029/2011JD016048>
- Xu, T., Bateni, S. M., Margulis, S. A., Song, L., Liu, S., & Xu, Z. (2016). Partitioning evapotranspiration into soil evaporation and canopy transpiration via a two-source variational data assimilation system. *Journal of Hydrometeorology*, 17(9), 2353–2370. <https://doi.org/10.1175/JHM-D-15-0178.1>
- Yu, X., Duffy, C., Baldwin, D. C., & Lin, H. (2014). The role of macropores and multi-resolution soil survey datasets for distributed surface-subsurface flow modeling. *Journal of Hydrology*, 516, 97–106.
- Zhao, W.-Z., Ji, X.-B., Kang, E.-S., Zhang, Z.-H., & Jin, B.-W. (2010). Evaluation of Penman-Monteith model applied to a maize field in the arid area of Northwest China. *Hydrology and Earth System Sciences*, 14(7), 1353–1364. <https://doi.org/10.5194/hess-14-1353-2010>
- Zi, T., Kumar, M., Kiely, G., Lewis, C., & Albertson, J. (2016). Simulating the spatio-temporal dynamics of soil erosion, deposition, and yield using a coupled sediment dynamics and 3D distributed hydrologic model. *Environmental Modelling & Software*, 83, 310–325. <https://doi.org/10.1016/j.envsoft.2016.06.004>

SUPPORTING INFORMATION

Additional supporting information may be found online in the Supporting Information section at the end of this article.

How to cite this article: Chen X, Kumar M, D deB Richter, Mau Y. Impact of gully incision on hillslope hydrology. *Hydrological Processes*. 2020;1–19. <https://doi.org/10.1002/hyp.13845>